Developing lab on a chip technology for the detection and characterisation of *Giardia duodenalis* cysts and *Cryptosporidium* spp. oocysts on foods

Kyle Ganz

A Thesis Submitted to the School of Graduate Studies
University of Ottawa

In Partial Fulfillment of the Requirement for the Degree of Master of Science

Department of Biochemistry, Microbiology and Immunology, Faculty of Medicine

ABSTRACT

In the present study methods which can be integrated into a complete lab on a chip system for the detection and characterisation of *Giardia duodenalis* cysts and *Cryptosporidium* spp. oocysts from foods were developed and tested. Microfluidic chips, which make use of inertial separation, were designed and fabricated for the concentration and separation of either cysts or oocysts from food particles. These chips were highly specific for their intended target and were shown to be effective when used for artificially contaminated lettuce samples. The quantification by real-time PCR of *Cryptosporidium* spp. hsp70 mRNA, expressed in response to a heat stress, was assessed as a potential lab on a chip method for the detection of viable oocysts from foods. This method proved to be effective in determining the viability of oocysts in apple cider and the effects of high hydrostatic pressures on the viability of oocysts.

ACKNOWLEDGEMENTS

First and foremost, I would like to thank my supervisors Dr. Brent Dixon and Dr. Jeffrey M. Farber for providing me with the opportunity to learn how to conduct proper scientific research in the field of food microbiology. Dr. Farber's constant challenges forced me to perform at my best and truly obtain a wide knowledge base in the field of microbiology. Dr. Dixon taught me how to properly communicate my work both at international conferences and in my writing, as well as provide me with in depth knowledge of protozoan parasites. I would also like to thank them both for their career guidance.

Secondly I would like to thank Dr. Teodor Veres, Senior Research Scientist and Group leader, and Dr. Liviu Clime, Research Scientist in the Life Sciences Division at National Research Council Canada, Boucherville, Quebec. Without their extensive collaboration, guidance and funding the inertial separation microfluidics project would not have been possible.

I would like to thank all the members of my Parasitology Laboratory at the Bureau of Microbial Hazards, including Ryan Boone, Harriet Merks, Asma Iqbal and Lorna Parrington, who have helped me with various methodologies and techniques. I would also like to thank both Nathalie Corneau and Christian Luebbert of the Research on Emerging Technologies Laboratory at the Bureau of Microbial Hazards who helped bridge my knowledge of food microbiology with novel rapidly emerging technologies. I would also like to thank Dr. Alex Gill for his instruction and guidance in performing the high pressure processing work.

Thank-you to all my thesis advisory committee members, Dr. Sean Li, Dr. Burton Blais and Dr. Liviu Clime for their time and advice.

Lastly, but most importantly I would like to thank my parents, Dr. Peter R. Ganz and Katherine Ganz, as well as Rebecca Rochman, for their ever-lasting support, love and confidence in me.

TABLE OF CONTENTS

LIST OF ABBREVIATIONS

A-T: Adenine-Thymine

cDNA: Complement DNA

DAPI: 4’,6-diamidino-2-phenylindole

FDM: Foci detection method

FITC: Fluorescein isothiocyanate

HCT: *Homo sapiens* colon ileocecal tissue

HPP: High pressure processing

hsp: Heat shock protein

IMS: Immunomagnetic separation

I: Inlet

ID50: 50% infectious dose

LC: Large channel

LOD: Limit of detection

MDCK: Madin-Darby canine kidney

mRNA: Messenger RNA

NTC: No template control

PBS: Phosphate-buffered saline

PCR: Polymerase chain reaction

PDMS: Polydimethylsiloxane

PES: Polyester

PI: Propidium iodide

PMA: Propidium monoazide

qPCR: Quantitative PCR

Re: Reynolds number

rRNA: Ribosomal ribonucleic acid

RT: Reverse transcriptase

RT-PCR: Reverse transcription PCR

SC: Separation channel

SD: Standard deviation

TPE: Thermoplastic elastomers

USEPA: United States Environmental Protection Agency

UV: Ultra-violet

LIST OF FIGURES AND ILLUSTRATIONS

LIST OF TABLES

1.0 GENERAL INTRODUCTION – *Cryptosporidium* spp. and *Giardia duodenalis* and their detection and viability in foods.

1.1 Significance of *Cryptosporidium* spp. and *Giardia duodenalis*

Giardia duodenalis (syn. *G. intestinalis, G. lamblia*) is an enteric protozoan parasite which infects a wide range of hosts, including humans and a variety of domestic and wild mammals. It is the most commonly identified intestinal parasite worldwide (29, 38), with an estimated 2.8 x 10^8 human cases of giardiasis annually (36). *G. duodenalis* prevalence is much higher in children than adults, and in developing than developed countries (20).

Cryptosporidium is a genus of enteric protozoan parasites that is currently made up of approximately 25 different species and 40 various genotypes (62). While some *Cryptosporidium* species are host-specific, others may infect a variety of different hosts. Several of the latter species are common to both humans and animals and may be transmitted zoonotically. For example, *C. hominis* is specific to human infection, while *C. parvum* can infect humans as well as a number of other mammals including cattle, goats, sheep and deer (19). *C. hominis* and *C. parvum* make up the majority of human cryptosporidiosis infections.

Transmission of both *G. duodenalis* and *Cryptosporidium* spp. involves the ingestion of the environmentally robust (oo)cyst, either directly by means of the fecal-oral route (person-to-person or zoonosis), or indirectly through (oo)cyst contaminated water or food. Ingestion of the (oo)cysts and subsequent infection by the parasites can lead to giardiasis or cryptosporidiosis, respectively. The infectious dose of *G. duodenalis* and *C. parvum* able to cause an infection in greater than 50% of immunocompetent humans was determined to be 10 cysts (59) and 132 oocysts, respectively (18). Infection in an immunocompetent host generally leads to either an asymptomatic infection or a self-limiting (acute) infection in which the host exhibits diarrhoea,

weight loss, abdominal discomfort and nausea (11). Cryptosporidiosis has also been associated with fever (40).

The complete pathophysiology behind the symptoms of giardiasis is still relatively unknown, however, it is known that *Giardia* trophozoites promote excessive enterocyte apoptosis, disrupt intestinal barrier function and cause a shortening of microvilli along the small intestinal epithelium (11). *Cryptosporidium* spp. infection has also been shown to cause apoptosis of epithelial cells lining the small intestine, disruption of barrier function, and also the production of an enterotoxin (40). While *Giardia* infection is largely confined to the small intestine, severe cases of *Cryptosporidium* infection can lead to extraintestinal sites of infection. Slight differences in the clinical manifestations of various *Cryptosporidium* species and even subtypes have been found (40). In children less than five years of age, chronic cryptosporidiosis infection can be very severe and lead to retardation of growth and development. Globally, one in 10 children die as a result of diarrhoeal disease in the first five years of life (45). As a result of this, many organizations, including the Bill and Melinda Gates foundation, have funded projects investigating the causative agents of diarrhoeal diseases. The global enteric multicenter study (GEMS) is one such study, which enrolled 9,439 children with moderate-to-severe diarrhoea at four locations in Africa and three locations in Asia over a three year period. This study reported that *Cryptosporidium* spp. was the second most common cause of diarrhoea (35). *Giardia duodenalis* was also identified as a causative agent, however, to a lesser degree. Cryptosporidiosis can also be very severe in the immunocompromised such as HIV-infected individuals, due to a depressed cell-mediated immunity.

1.2 *Giardia duodenalis* life cycle

Following ingestion, *G. duodenalis* cysts are exposed to various environmental cues in the host's gastrointestinal tract. Exposure to H+ ions and low pH in the stomach followed by exposure to the more neutral pH in the duodenum of the small intestine, triggers the excystation of the cysts (8). Excystation is the process in which the cyst's membrane ruptures allowing for the release of undivided trophozoites which each contain two nuclei (54). Immediately following the release of the trophozoite, cytodifferentiation and cytokinesis occurs giving rise to two daughter trophozoites each containing two nuclei (Figure 1). The trophozoite life stages have four pairs of flagellae and are thus motile. They are able to adhere to epithelial cells in the host's small intestine through their ventral adhesive disc (Figure 2), however, attachment is not a necessary step for completion of the life cycle or for the uptake of nutrients. It is thought that high levels of bile in the upper small intestine stimulate the encystment of the trophozoite (24, 71). The cyst wall maturation and duplication of the nuclei occur during subsequent passage through the lower gastrointestinal tract giving rise to fully infectious cysts that are shed with the host's feces (54).

1.3 *Cryptosporidium* spp. life cycle

Cryptosporidium spp. has a very complex life cycle involving both sexual and asexual phases and is thus found in a variety of life stages. In the environment, *Cryptosporidium* is mainly found in its oocyst stage which is excreted with the feces of infected hosts. The oocyst wall itself is a trilaminar structure (26) whose purpose is to provide the four inner sporozoites with protection from the harsh environment outside the host. Oocysts of *C. parvum* have been shown to be extremely resistant to a number of commercial disinfectants used at high concentrations which would normally be effective in killing most microorganisms (19).

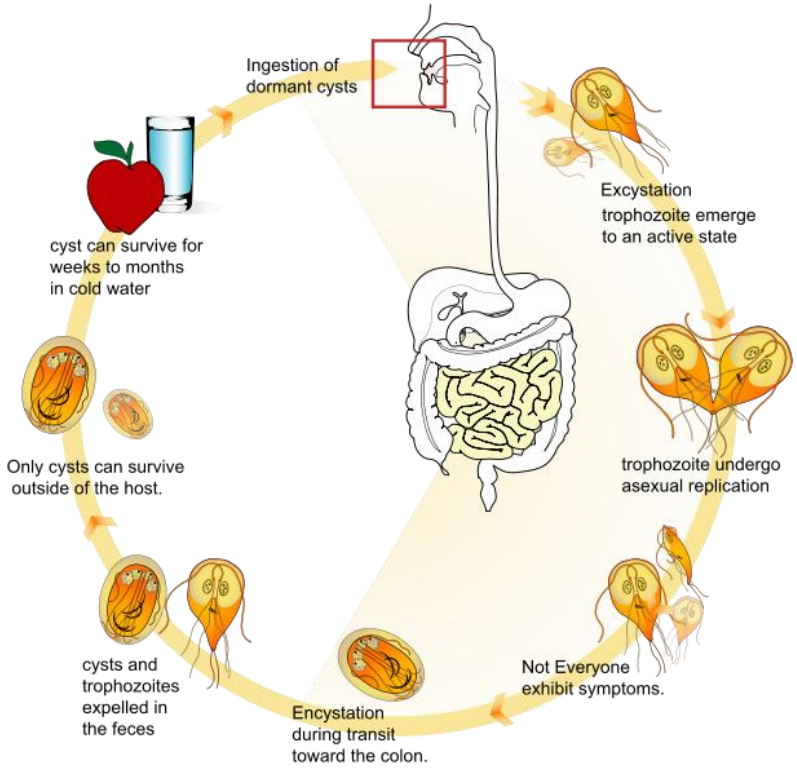

(http://en.wikipedia.org/wiki/Giardia_lamblia#mediaviewer/File:Giardia_life_cycle_en.svg. Not copy righted by author; author grants anyone the right to use this work for any purpose, without any conditions; accessed 2014; last updated 2008.)

Fig. 1 *Giardia duodenalis* life cycle. Illustration of the various developmental stages of *G. duodenalis* in an infected mammalian host. Upon exposure to environmental cues from the host's small intestine, the ingested cyst excysts in an active trophozoite state which contains four nuclei. With its nuclei already duplicated, binary fission is able to take place almost immediately, creating two trophozoites, each with two nuclei. During transit towards the colon, encystation of the trophozoite can take place, allowing for the return to its environmentally robust cyst form and completion of the life cycle.

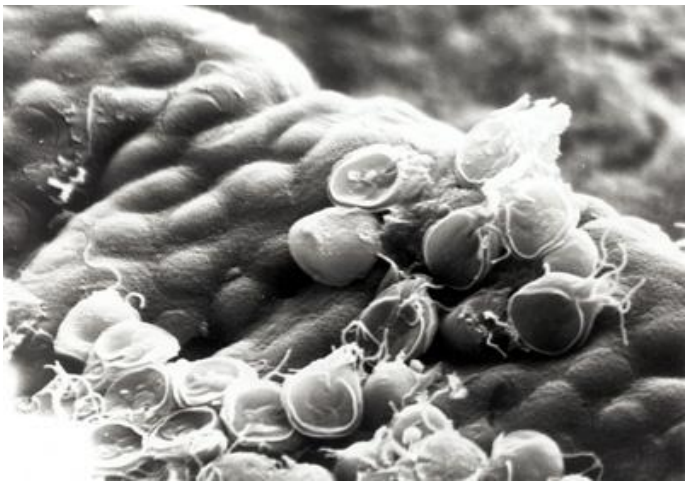

Fig. 2 *Giardia* trophozoite infection. Scanning electron micrograph of the intestinal villi of a severe combined immunodeficient mouse infected with *Giardia muris*. The oval-shaped cells, either adhering or surrounding the villi, containing four pairs of flagellae and a flat ventral adhesive disk are *Giardia* trophozoites.

Upon ingestion by its host and subsequent travel through the host's gastrointestinal tract, the oocyst receives a number of environmental cues. Excystation, the process by which the oocyst wall coils inwards and opens to allow for the inner sporozoites to be released, is triggered by environmental cues found in the stomach and small intestine such as bile, low pH, temperature and certain proteases. The sporozoite life stage of *Cryptosporidium* spp. is motile and is able to bind to host epithelial cells through ligand-receptor mediated interactions (77). Upon attachment, the sporozoite triggers the rearrangement of the host's actin cytoskeleton to encompass it within the host cell membrane. This enveloping process, along with the formation of a cluster of vacuoles at the host-parasite interface, forms what is referred to as a parasitophorous vacuole, which encompasses the sporozoite (80). Therefore at this stage in the infection, the parasite is intracellular but extracytoplasmic (84). This host-parasite complex can now allow for the formation and attachment of a feeder organelle, and with it the uptake of nutrients by the parasite. As this process in infection progresses, the sporozoite life stage of *Cryptosporidium* spp. transforms into a trophozoite life stage (Figure 3). Asexual reproduction is able to occur at this stage of infection. The duplication and division of the *C. parvum* nucleus into 6 or 8 nuclei contained in individual merozoites occurs in what is called a type I meront (Figure 3). These newly created merozoites are very similar to the sporozoite life stage in that they are able to infect new host epithelial cells and undergo additional rounds of asexual reproduction. The infection of a new host cell by the merozoite can create a type II meront, which is able to produce four merozoites. The merozoites developed from a type II meront are able to begin the sexual reproductive phase of the life cycle. They can infect new host cells and develop into an undifferentiated gamont which can further develop into either a microgamont (male) or macrogamont (female). Microgametes are formed from the microgamont and can fertilize the

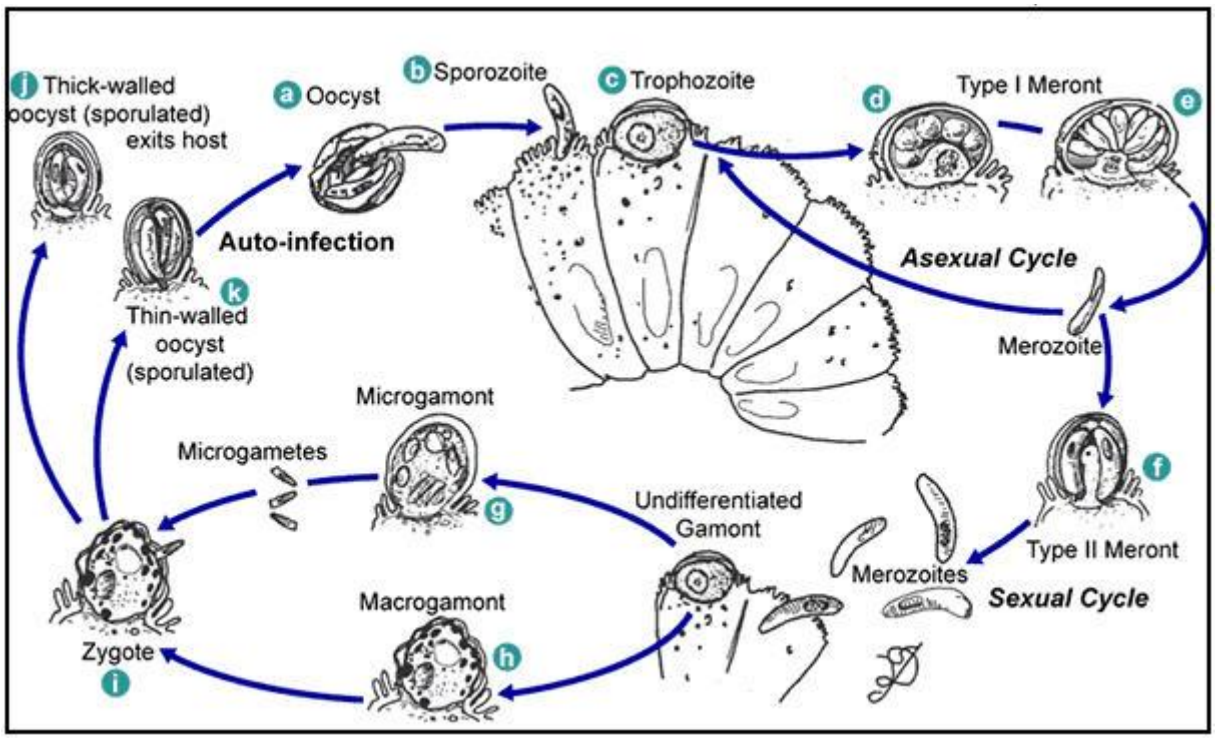

Fig. 3 *Cryptosporidium parvum* life cycle. Illustration of the various developmental stages of *C. parvum* in an infected mammalian host. Upon exposure to environmental cues from the host's small intestine, the ingested oocyst excysts (a), allowing for the four inner sporozoites (b) to be released where they can adhere to epithelial cells of the small intestine. Following attachment, the sporozoite and host cell form a parasitophorous vacuole in which nutrients can be taken up by the growing parasite. At this point, the parasite is in its trophozoite (c) life stage and is uninucleate. Upon asexual reproduction, the organism is called a type I meront, and they can contain between 6 (d) and 8 (e) merozoites. The merozoites are a very similar life stage to the sporozoites and are able to infect new host cells and form a type II meront (f). Type II meronts undergo asexual reproduction to produce more merozoites. Upon infection of new host cells by the merozoites produced from a type II meront, an undifferentiated gamont is formed. This undifferentiated gamont can further grow into either a microgamont (male) (g) or macrogamont (female) (h). Sexual reproduction can occur when microgametes, produced from the microgamont, fertilize a macrogamont forming a zygote (i). The zygote forms either a thin-walled oocyst (k), which can re-infect host cells and undergo another life cycle, or a thick-walled oocyst (j), which is shed into the environment with the host's feces.

female macrogamont to create a zygote. The zygote can then develop into either a thin-layered oocyst or a thick-layered oocyst, the latter of which is the stage that is shed into the environment with the host's feces. The thin-layered oocyst can remain in the intestinal tract and excyst once more leading to re-infection.

1.4 *Cryptosporidium spp.* and *Giardia duodenalis* association with foods

The majority of cryptosporidiosis and giardiasis outbreaks are waterborne (drinking and recreational water). A review by Karanis et al. (31) summarised global protozoan parasite outbreaks that took place up until the year 2003, and identified 132 and 165 waterborne outbreaks of *G. duodenalis* and *C. parvum*, respectively. Although foodborne transmission is not as important as waterborne or fecal-oral (person-to-person) transmission in terms of numbers of cases or outbreaks, it is an emerging issue especially in developed countries. It is currently estimated that 8% and 7% of cryptosporidiosis and giardiasis cases, respectively, in the US are foodborne (69). Contamination likely occurs at the farm level as livestock act as reservoirs for both *C. parvum* and *G. duodenalis.* Calves infected with *C. parvum* can shed up to 6×10^7 oocysts per gram of feces into the environment (79) and a recent study performed in 15 dairy farms in the US determined that the prevalence of *Cryptosporidium* in 0-11 month-old calves was 35.5% (68). The shedding of such high numbers of parasites into the environment may lead to the spread of cysts or oocysts to downstream farms. Thus, foods such as produce may become contaminated with cysts or oocysts via contact with contaminated manure, agricultural runoff or fecal-contaminated irrigation water. Contamination of food products by humans can also occur during the harvest, packaging, transport or food preparation processes. *C. hominis* and *G. duodenalis* may also be transmitted by food though infected food handlers. Foods that have

previously been reported to be contaminated with *C. parvum* or *C. hominis* oocysts include fresh fruits and vegetables, raw milk, oysters and apple cider (62). Foods that have previously been reported to be contaminated with *G. duodenalis* cysts include fresh fruits and vegetables, shellfish, and more recently meats (10). Fresh fruits and vegetables contaminated with *G. duodenalis* cysts and *Cryptosporidium* spp. oocysts are of particular public health concern as they are generally consumed raw and often originate in developing countries with lower standards of water quality and hygiene. An overview by Roberston of foodborne outbreaks which occurred between the years of 1984 and 2012 (62) identified a total of 30 giardiasis and cryptosporidiosis outbreaks. A summary of the reported incidence of both protozoan parasites was tabulated by Dixon (16) and included 16 *Cryptosporidium* studies with prevalences ranging from 0.6 – 63%, and 38 *Giardia* studies with prevalences ranging from 0.9-83.3%. One of these reports was a surveillance study performed in Ontario, Canada on ready-to-eat packaged leafy greens, which identified *Cryptosporidium* oocysts on 5.9% and *Giardia* cysts on 1.8% (n=544) of samples. Another of these studies investigated the occurrence of parasites on fruits and vegetables in Norway (64), and found either *Giardia* cysts and *Cryptosporidium* oocysts on 6% (n=475) of the total samples.

1.5 Detection of protozoan parasites on foods

Each food matrix provides its own unique challenge during testing, and there is currently no standard methodology for the isolation of *G. duodenalis* cysts or *Cryptosporidium* spp. oocysts from foods. Available methods generally involve the elution of the (oo)cysts from the surface of the food, the concentration of the (oo)cysts, and finally their detection.

1.5.1 Elution and Concentration

The elution of the (oo)cysts from the surface of the food through the use of an elution buffer (pH buffer and detergent) and an orbital shaker or rocker, results in a parasite suspension which contains a low concentration of the desired parasites and a high concentration of interfering food particles with more fragile food matrices containing higher amounts of interfering food particles. Unlike with most foodborne bacteria, where an enrichment step can be used to enrich the organism and lower detection limits, current *G. duodenalis* and *Cryptosporidium* spp. axenic (no host organisms) culture methods have had limited success with pure suspensions of *G. duodenalis* cysts. Growth was much slower than most foodborne bacteria with generation times between 6-12 hr (2). As a result, the parasites must be concentrated to allow for their detection. The success of the detection methods is correlated to the efficiency of these methods in recovering and concentrating the (oo)cysts from the food samples. The concentration of parasites from large volumes is usually performed by centrifugation. However, all the food particles present in the suspension are also concentrated (pelleted) by this method. Initial filtration of the suspension can be performed to remove the larger food particles, however, as the (oo)cysts range in size from 3-10 µm (12), many of the smaller food particles cannot be removed without the loss of parasites.

Immunomagnetic separation (IMS) is a concentration and separation technique patented in 1980 by Senyei and Widder. The patent encompasses the separation of cells, bacteria, or viruses through the use of microspheres containing magnetic particles that are coated with antibodies. A number of assays specific for a range of bacterial and parasitic microorganisms have been developed and commercialized for use in detection methods. The United States Environmental Protection Agency (USEPA) methods 1622 and 1623, which are currently the only standardized and validated detection methods for *Cryptosporidium* oocysts and *Giardia* cysts in water

samples, use an IMS step to help concentrate and separate out the parasites from a heterogeneous aqueous matrix. This IMS step has also been integrated into a number of food detection methods such as that of Robertson and Gjerde (63), and Cook et al. (14) in an attempt to try and reduce the number of food particles in the final parasite concentrate. This method is not as effective for use with food samples, as many food particles found in the elution suspension may inhibit epitope-paratope interactions, or may non-specifically bind to antibodies. Recovery efficiencies in turbid solutions may be as low as 60% (Dynabeads GC-Combo, Life Technologies, Norway). The IMS step is also time-consuming, requiring at least 1 hr of antibody binding followed by additional wash and dissociation steps. In addition, the majority of the monoclonal antibodies have been raised against a limited number of *Giardia* and *Cryptosporidium* isolates and may not be effective at recognizing epitopes on all species and genotypes (76). Lastly the IMS kits are also costly, thus a number of in-house methods forgo the use of IMS in their elution and concentration methods.

1.5.2 Detection

The gold standard method for the detection of both *Cryptosporidium* spp. oocysts and *G. duodenalis* cysts is immunofluorescence microscopy, in which commercially available fluorescently-labeled monoclonal antibodies specifically targeting the (oo)cyst wall are used. Flow cytometry can similarly be used; however, its accuracy decreases as the number of parasites in the solution decreases and the number of background particles increase. This is due to non-specific binding of the antibodies to food particles of similar size to the (oo)cysts themselves, or food particles of similar target size autofluorescing. These are difficult to gate out (isolate a specific group of cytometric events from a larger set) in the flow cytometry analysis and are difficult to confirm, as no morphological assessment can be made as in microscopy.

Imaging flow cytometry, which combines the speed benefits of flow cytometry with the imaging of microscopy, appears to be a better approach, allowing for visual confirmation of the particles/events.

Polymerase chain reaction (PCR) is also often used in detection, and is particularly useful in performing further molecular epidemiology and typing of organisms. Dixon et al. (17), for example, performed a two-step nested PCR of a fragment of the 18S rRNA *Cryptosporidium* gene and the 16S rRNA *Giardia* gene as an initial sample screening step. An initial PCR screen for the organisms allows for the rapid identification of contaminated samples, which can be further analyzed by fluorescence microscopy to confirm the presence of intact (oo)cysts. DNA extraction from the robust cyst is difficult, however, and PCR inhibitors in foods may reduce the sensitivity or inhibit amplification all together.

Samples with large numbers of food particles increase the *Giardia* and *Cryptosporidium* detection limits and analysis times of all the above mentioned detection techniques. Food particles are capable of inhibiting the formation of the antigen-antibody complex necessary in immunofluorescence detection methods, by obstructing or chemically altering the epitope region where binding occurs. These food particles may also non-specifically bind the fluorescently-labeled antibodies which may lead to the detection of false-positives during immunofluorescence microscopy or flow cytometry as described above. Larger food particles may also hide or obstruct (oo)cysts during microscopic examination preventing their identification/detection. A number of PCR inhibitors such as polysaccharides, pectin, polyphenols, phenols, glycogen and xylans have been found in foods that are known to be contaminated with *G. duodenalis* including lettuce, berries and shellfish (51, 70). Thus, developing better concentration and purification methods that reduce the number of food particles in the final parasite preparation, while

obtaining a high recovery of parasites, are key to improving the overall detection of (oo)cysts from foods.

1.6 Determining the viability of *Cryptosporidium* and *Giardia*

Determining the prevalence of *G. duodenalis* and *Cryptosporidium* spp. (oo)cysts in food products is important in determining the health risks associated to the public. It is also important that an accurate health risk assessment include an estimate of the viability and/or infectivity of the (oo)cysts. When the (oo)cysts are shed from their infected host into the environment, they contain all the necessary biological characteristics needed for infection. Although the (oo)cysts are very robust and can survive for extended periods in damp and cool conditions, their viability and infectivity is still limited to a couple of months (62). A study investigating the viability of *Cryptosporidium* and *Giardia* (oo)cysts in water, soil and cattle feces at -4°C, 4°C or 25°C found that they could survive for greater than 12 weeks in all three matrices at -4°C and 4°C, and between 8-12 weeks at 25°C (55). This determination was made using propidium iodide (PI) as a viability marker. The same study also determined through the use of animal models that infectivity of the oocysts and viability of the oocysts correlated with each other; however, the oocyst infectivity decreased slightly more rapidly than their viability. Therefore, it is possible that viable oocysts may not be infectious.

Cell culture or animal infection models are current methods used in assessing infectivity, while excystation and dye permeability assays are currently being used for assessing the viability of both *Cryptosporidium* and *Giardia* (oo)cysts. (Oo)cysts that are no longer viable or infectious may be detected by molecular detection methods such as PCR, or may still have intact walls which can bind antibodies during immunofluorescence microscopy or flow cytometry. Most prevalence studies on foodborne parasites do not include viability or infectivity determinations as

most of the current methods, as discussed in detail below, are not suitable. Ideally an accurate, sensitive, cost-effective, high-throughput and rapid viability and/or infectivity assay is needed, which can preferably be integrated into a lab on a chip system used in the routine detection of parasites on foods. An ideal method such as this would also allow for a more accurate health risk assessment of contaminated food samples and also allow one to assess the effectiveness of disinfection/sterilization treatments used in food processing.

1.6.1 Axenic culturing

Unlike most microbiological detection methods which make use of cell culture techniques to enumerate the number of viable cells present in a food sample, most parasites are host dependent and require a specific host for reproduction.

Giardia was shown to be culturable axenically (host cell-free) in the 1970s by E. A. Meyer (50). Following this discovery, in 1980, Diamond et al. (23) found that a medium originally developed for the cultivation of *Entamoeba* and trichomonad species (TYI-S-33) could also be used to support the axenic growth of *Giardia in vitro*. A few years later D.B. Keister (32) modified the TYI-S-33 medium, primarily by adding bile, to produce the medium which is commonly used today to support the axenic growth of a number of *Giardia* species.

In 2004, Hijjawi et al. (28) published the first report indicating the successful axenic cultivation of *C. parvum*. This report was met with a lot of skepticism. *Cryptosporidium* spp. was thought to be un-culturable in a cell-free system due to its more complex life cycle (Figure 3), consisting of both asexual and sexual stages, along with its many intracellular life cycle forms. In 2006, Girouard et al. (25) published a response article in which they determined that the oocysts did not complete their life cycle and produce new, viable or infectious oocysts (25). However, since then, Hijjawi et al. published additional articles supporting their original work, including

one in 2010 (27) in which they successfully demonstrated the growth of *C. hominis* through qualitative PCR (qPCR) analysis, which revealed a 5 to 6 fold amplification of parasite DNA.

Unlike with most bacteria, however, growth (or multiplication) of parasites in these cell-free cultures takes much longer, with generation times of 6-12 hr for *G. duodenalis* (2) and doubling-times of 3-4 days for the cultivation of *Cryptosporidium* spp. (27). The methods are also quite laborious, e.g., the cultivation of *Cryptosporidium* spp. requires numerous treatments and steps including; purification of the oocysts, excystation, purification of the sporozoites, and culturing for days (27). Therefore, although these methods are crucial in the study of cell biology, host-parasite interactions, and pathology, they are not suitable for routine viability and detection methods.

1.6.2 Excystation and dye incorporation viability assays

G. duodenalis cysts and *Cryptosporidium* spp. oocysts contain all the necessary components for infection immediately following their excretion from an infected host. Their robust (oo)cyst wall protects the inner trophozoites or sporozoites from the harsh environment and maintains their infectivity for an extended period of time. Therefore, the ability of (oo)cysts to excyst and release the infectious life forms have been correlated with the viability of the (oo)cyst. *In vivo* excystation of *G. duodenalis* cysts and *Cryptosporidium* spp. oocysts is triggered by environmental cues arising from the host's small intestine. *In vitro* conditions for the excystation of *G. duodenalis* cysts, allowing for the release of the two inner trophozoites, were initially defined in 1979 by Bingham & Meyer (9). The conditions for *in vitro* excystation of *C. parvum* oocysts were examined in 1987 by Woodmansee (85). Since then, a number of excystation conditions have been determined that mimic host-derived signals such as temperature, bile salts, pH, proteases and reducing agents (77). By microscopic enumeration of

the number of sporozoites/trophozoites, empty shells, and partially excysted and non-excysted cysts or oocysts following an excystation treatment, an estimate of the percent of viable parasites in a sample can be determined. However, this method is technically difficult, as microscopy must be performed without the aid of fluorescent antibodies for the sporozoite/trophozoite, and identification of the sporozoites requires extremely high magnification (>400X). In addition, the high number of background food particles which are found in parasite concentrates collected from foods, can make enumeration in bright field very difficult.

Another rapid and cost-effective assay used to determine the viability of *G. duodenalis* cysts and *Cryptosporidium* spp. oocysts, which is commonly used in cell biology, involves the use of vital dyes, in particular, PI and 4',6-diamidino-2-phenylindole (DAPI). PI can pass through cell walls which lack integrity (i.e., compromised) and bind to nucleic acids such as DNA or RNA. Thus, the presence of stain in the nuclei of the (oo)cyst indicates that the parasite is non-viable. DAPI binds to A-T rich regions of DNA and can pass through intact cell membranes. Distinguishing between viable and non-viable (oo)cysts with DAPI is difficult, however, as viable cells are stained primarily within the nucleus, indicating that the nuclear membrane is intact, while non-viable (oo)cysts are stained primarily in the cytoplasm. These vital dye assays are known to over-estimate the viability of both *G. duodenalis* cysts and *Cryptosporidium* spp. oocysts (65). In addition, the lack of integrity of the (oo)cyst wall does not necessarily mean that the inner trophozoites/sporozoites are non-viable.

1.6.3 Foci detection method infectivity assay

A number of *in vitro* cell culture methods were initially developed to determine the infectivity of *C. parvum* oocysts as they require cell attachment for reproduction. These methods make use of a number of different cell lines, such as, Madin-Darby canine kidney (MDCK) cells

or the human epithelial intestinal cell line (HCT-8) with various complementary growth conditions. Most methods typically involve an initial excystation step in which the oocysts are exposed to trypsin, bile and/or sodium hypochlorite at 37°C (81). The excysted oocysts are then incubated along with the cell monolayer at 37°C for a number of days. Polyclonal antibodies specific for various life cycle forms of the parasite are incubated with the cell monolayer and examined microscopically for indications of successful infection of the host cells. The foci detection method (FDM), developed by Slifko et al. in 1997 (73), is currently the most widely used *in vitro* infectivity assay. Through dilution studies, levels as low as one infectious oocyst was detected, and the assay correlated with the available viability assays (73). This *in vitro* assay is time-consuming, however, as it requires growth of the epithelial cell monolayer for 48 hr, followed by another 48 hr incubation period with the excysted oocysts. Detection is also time consuming, as infected foci must be enumerated by fluorescence microscopy. The method is fairly expensive as it requires the constant maintenance of the epithelial cell line as well as the purchase of labeled-antibodies for the detection of the infected foci. It is also difficult to obtain accurate quantitative data on the number of infectious oocysts in a sample, as four sporozoites are released from each oocyst during excystation, thus allowing anywhere from 0-4 foci to develop on the cell monolayer per infectious oocyst. In addition, the high number of background food particles which are found in parasite concentrates collected from foods has been shown to interfere with the enumeration (74).

1.6.4 Animal infectivity assays

The gold standard for determining viability and infectivity is through the use of animal models. A review of the many animal models used to study gastrointestinal infection of *C. parvum* is outlined by Lindsay et al. (43). Although a number of mammals such as hamsters,

guinea-pigs, cats, dogs and calves are used, the most commonly used animals are mice and rats. While immunocompetent adult mice and rats are resistant to infection, nursing mice and rats are susceptible and are, thus, the most useful in determining the infectivity of low doses of oocysts. The oral 50% infectious dose (ID50) for *C. parvum* in suckling BABL/c mice, for example, is 60 oocysts (34). *C. hominis* infection was eventually obtained in calves, and newborn lambs and pigs (1, 22); however, longer prepatent (the period between infection and recovery of an infective form from the blood or feces) were observed in comparison to *C. parvum* infection. In 2005, Baishanbo et al. (4) demonstrated infection in immunosuppressed Mongolian gerbils, which proved to be a more ideal model. *Giardia duodenalis* Assemblages A and B, which infect humans, have similarly been shown to be infectious in suckling mice (48) and gerbils (46). Animals are usually inoculated with (oo)cysts orally, with infection determined through examination for (oo)cysts in the stool or through intestinal examination post-mortem (13, 37). Using animal models to assess infectivity, however, is very labour intensive and time consuming as the animal's intestines are examined 5 to 11 days post-infection, to allow time for the parasites to make their way to the small intestine and establish an infection (7, 13, 43). Animal models are also very costly and are associated with a number of ethical issues.

1.6.5 Hsp70 mRNA viability assay

The heat shock protein (HSP) 70 family are a group of proteins related in structure and function that are involved in a number of different roles in the cell including post-translational protein assembly, folding, translocation and most importantly in helping protect the cell from stress (6). Upon exposure to a stress, viable and thus metabolically active organisms are able to up-regulate the transcription of hsp70 mRNA for eventual translation into the hsp70 protein. The hsp70 expression has been predominantly studied in *Drosophila* where it was originally

discovered by Ritossa in 1963(61). In *Drosophila* cells, it was demonstrated that hsp70 mRNA is transcribed in very high numbers in response to heat shock (2-3 min following induction). It was also found that its expression was repressed immediately following the stress and, more importantly, the mRNA that was produced was degraded in a highly regulated fashion (58).

In 2009, Garces-Sanchez et al. (21) developed a viability assay which correlates the amount of hsp70 mRNA produced during a 20 min heat shock at 45°C to the amount of viable *C. parvum* oocysts present in a sample. This viability assay is performed by using quantitative real-time reverse transcription PCR (qRT-PCR) to quantify the levels of hsp70 mRNA. This allows for rapid and high-throughput viability studies to be performed in contrast to time-consuming cell culture or animal infection models for determining infectivity, or the excystation and dye permeability assays for determining viability. The researchers designed the primer and probe set to be specific for both *C. hominis* and *C. parvum,* and to amplify a 144 bp region close to the center of the gene.

In 2010, Bajszar and Dekonenko (5) realized the potential use of this assay in studying the viability of *C. parvum* following treatments with inactivation agents. They examined the response of stress-induced hsp70 gene expression and *C. parvum* oocyst inactivation by chlorine-based oxidants. Hsp70 mRNA proved to be an ideal target in comparison to β-tubulin and 18S rRNA markers, as the hsp70 mRNA transcript was degraded at a rapid rate following its induction, as determined by a 72 hr time course assay. Hsp70 mRNA expression was induced in response to the chlorine-based oxidants, similar to the response observed to heat. Approximately 24 hr following treatment, greater than 90% of the induced hsp70 mRNA transcripts were degraded. Thus, one day following treatment, the viability of the oocyst population was assessed

as the hsp70 transcripts returned to basal levels. This study ultimately found that a 4 hr exposure to 200 mg/L of mixed oxidants reduced the viability of a 10^5 oocyst suspension by 3 log.

However, this viability assay has not been tested for oocysts in complex food suspensions which may contain inhibitory particles to the real-time PCR. This viability assay is extremely promising as it is rapid, accurate, sensitive, cost-effective and high-throughput, thus having the potential to be extremely useful in routine surveillance studies, or in foodborne outbreak investigations. As much progress is being made in integrating nucleic acid extraction and real-time PCR in microfluidic based devices, this hsp70 viability assay may be integrated into a complete lab on a chip detection system (53).

1.7 High pressure processing in the food industry

Most of the current inactivation treatments proven to be effective against *Cryptosporidium* have been designed for use in the treatment of water and include; irradiation, heating or freezing and chemical treatment (62). However, the need for a sterilization process which reduces the microbial load in foods, thus extending shelf-life, while minimally altering the nutritional content (e.g., vitamins), texture and flavour of food products, is also evident. Processes making use of traditional treatments such as a disinfectant wash, blast freezing, pasteurization and UV irradiation, have been integrated into the processing/manufacturing of certain foods (62). A more recent food specific technique called high pressure processing (HPP), which exposes the microorganisms to high hydrostatic pressures, has become a routine processing technique in the manufacturing of various food products.

Common pressures used in commercial systems vary between 400 MPa and 700 MPa. The high hydrostatic pressure is applied through the use of either a gas or liquid and is applied uniformly, thus allowing solid foods to maintain their shape (67). The gas or liquid is pumped

into a pressure vessel by a pressure intensifier, until the desired pressure is reached at which point the pressure is maintained for the desired length of the run (hold time). The food sample is placed in a heat sealed bag within the pressure vessel prior to starting a run. The majority of the research that has been performed has focused on the effects of high hydrostatic pressure on various bacterial pathogens such as *Salmonella*, *Escherichia coli*, and *Listeria.* Recent work by Klotz et al in 2010 (33) investigated the relationship between membrane damage, the release of protein, and loss of viability in various *E. coli* strains under high hydrostatic pressures. This author noticed a strong correlation between the loss of membrane integrity followed by the loss of protein within the cell, and eventual cell death. This technology is currently being applied to a number of food products such as jams, fruit juices, pourable salad dressings, raw squid, rice cakes, foie gras, ham, oysters and guacamole (82).

Chapter I – Enhancing the detection of *Cryptosporidium* spp. oocysts and *Giardia duodenalis* cysts on foods using inertial microfluidic separation

2.0 INTRODUCTION

2.1 Microfluidic inertial separation of microparticles

Inertial microfluidic separation is rapidly emerging as an efficient separation, filtration and concentration technology in biologics, due to its low cost, high-throughput, and lab on a chip potential. It has recently found application in the separation of nucleated cells (57), cancerous cells (39, 56, 78), and stem cells (30) from whole blood. It has also been used in the separation of *E. coli* from erythrocytes (86). Inertial microfluidic separation makes use of the hydrodynamic forces which act on particles within a fluid as it flows through a channel.

When a fluid is flowing through a closed channel, two types of flow may occur, either laminar (streamlined) flow, in which the fluid flows in parallel layers without lateral mixing, or turbulent flow, in which lateral mixing can occur in the form of eddies or swirls. Laminar flow occurs if inertial forces dominate, whereas turbulent flow occurs if viscous forces dominate. A dimensionless number termed the Reynolds number (Re) provides the ratio of inertial forces to viscous forces and dictates what type of flow will occur (60). At very high Re numbers (>2040), fluid motion will be turbulent (3). Microfluidic flows are often associated with low-moderate Reynolds numbers and negligible inertia, which can allow for micro particles in a suspension to follow fluid streamlines along the microfluidic device.

Experimental studies of flows in circular pipes have shown, however, that randomly dispersed and suspended particles flowing (in laminar flow) are able to cross streamlines and focus in a reproducible manner to a narrow annulus (“tubular pinch effect”) (Figure 4) of radius 0.6R where R is the radius of the pipe (72). Since the lateral force responsible for migrating the

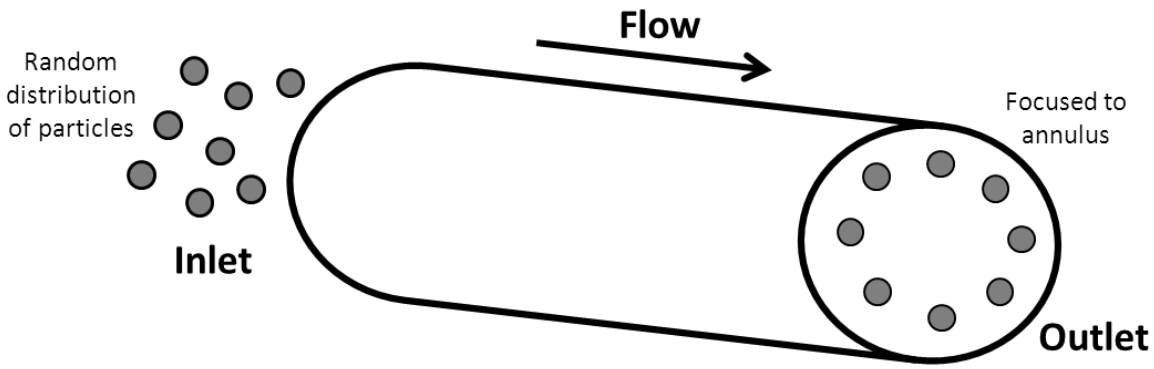
Flow
Random
distribution
of particles
Inlet
Focused to
annulus
Outlet

Fig. 4 Formation of an annulus occurs in a pipe under laminar flow. Segre and Silberberg (1961) observed that formation of an annulus upon flowing randomly distributed particles through a pipe. Prior to this discovery, it was thought that particles under laminar flow would follow their streamline through the entire channel. This discovery led to the findings of inertial forces which can act on particles under low to moderate Reynolds number and cause the lateral transfer of particles across streamlines.

particles toward the wall was found to be proportional to U^2 (where U is the fluid velocity), the effect was associated with the inertia of the fluid, which was confirmed later on by several other studies (49, 66, 83). The particles are driven to migrate laterally across the streamlines due to two inertial forces, the shear-induced lift force (Fs) and the wall-induced lift force (Fw) (Figure 5a). The shear-induced lift force pushes the particles towards the channel walls. This force arises from the velocity profile of the fluid as it flows (laminar flow) through a channel (pipe). The wall-induced lift force counteracts the shear-induced lift force and pushes the particles back towards the center of the channel (Figure 5a). This force arises from the flow of liquid around the particle as it approaches the wall, which induces a pressure increase between the particle and the wall (15). These opposing lift forces are dependent on the ratio of the particle size to the channel diameter. Particles that are at least 7% the size of the channel have been shown to be affected by these inertial forces and are subsequently ordered in equilibrium positions close to the channel walls (47). The focusing positions of the particles within the channel are mostly determined by the dimensions and shape of the channel itself. Thus, the number and location of equilibrium positions within a channel vary dependent on the geometry and size of the channel. Cylindrical, square and rectangular channels all focus particles at different locations (15). In rectangular microchannels for example, migration into two equilibrium positions close to the channel walls has recently been observed by Lim et al. (42) (Figure 5b). Focusing is also dependent on the length of the channel. Zhou and Papautsky (88) observed that in a 50 μm by 100 μm rectangular channel, containing particles ranging in size from 7.32-20 μm, the larger particles migrated much faster to equilibrium positions (1 mm downstream for the 20 μm particle) than the smaller particles (3 mm downstream for the 7.32 μm particle).

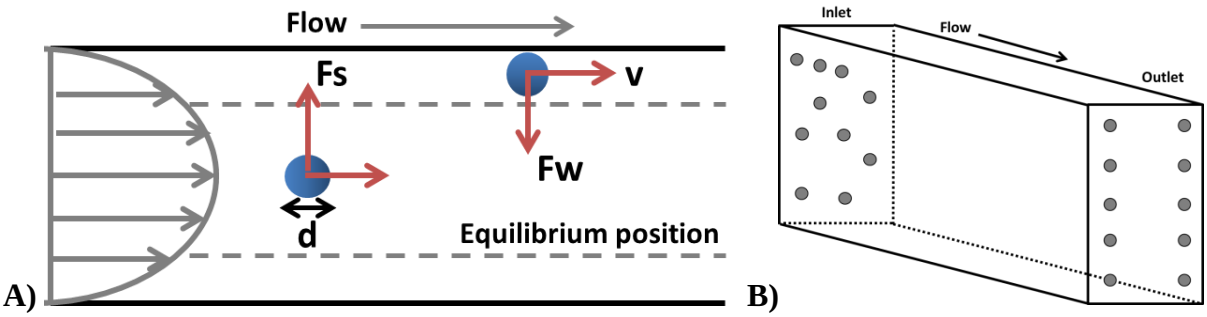
Flow
Fs
v
Fw
d
Equilibrium position
A)
Inlet
Flow
Outlet
B)

Fig. 5 Inertial focusing in rectangular microchannels. (A) The inertial forces that act on particles in laminar flow in a microchannel and order them in distinct equilibrium positions include the shear-induced force (Fs), which arises from the velocity profile of the fluid and pushes the particles toward the channel walls, and the wall-induced force (Fw), which arises from the flow of liquid around the particle as it approaches the wall and pushes the particles back towards the centre of the channel. Randomly distributed particles of specific diameters (d) under specific velocities (v) exhibit equilibrium positions (B) close to the rectangular channel's side walls as a result of these forces.

By manipulating the dimensions of a microchannel as well as the flow rate, particles of a desired size can be focused within the channel and separated from undesired smaller particles. Thus, particles such as *G. duodenalis* cysts or *Cryptosporidium* spp. oocysts could theoretically be targeted by designing and fabricating chips specific for particles ranging 6-10 µm or 4-6 µm in size. By designing a chip that captures the particles at the specific equilibrium positions, it is possible to separate out the desired particles from the undesired particles. This could theoretically be applied to passively isolate cysts or oocysts out of a suspension containing unwanted food particles without the need for specific antibodies, filters or centrifugation, and this could be done in a high-throughput passive manner which allows for rapid sample processing.

2.2 Hypothesis

Cryptosporidium spp. oocysts and *G. duodenalis* cysts can be concentrated and separated from suspensions containing food debris by microfluidic inertial separation. The integration of inertial separation chips into current methods for the elution and concentration of (oo)cysts will improve the speed, sensitivity and specificity of detection of *Cryptosporidium* spp. oocysts and *G. duodenalis* cysts on foods over those of existing methods.

2.3 Objectives

1. Obtain initial proof of concept of the microfluidic inertial separation of *Cryptosporidium* spp. oocysts and *G. duodenalis* cysts.

2. Demonstrate the ability of the microfluidic inertial separation chips to selectively concentrate (oo)cysts over smaller non-specific particles in suspension.

3. Develop a method integrating the microfluidic inertial separation chips for the elution and concentration of (oo)cysts from food.

4. Compare percent recoveries, limits of detection and sample homogeneity of a conventional detection method to the newly developed inertial separation method.

3.0 METHODS

3.1. Parasite isolates

Suspensions of *G. duodenalis* cysts and *C. parvum* oocysts were purchased from Waterborne, Inc. (New Orleans, LA). The human isolate H-3 *G. duodenalis* cysts were passaged through gerbils, purified from their fecal matter and suspended in phosphate-buffered saline (PBS) with antibiotics. The bovine isolate *C. parvum* oocysts were passaged through calves, purified from fecal matter and suspended in PBS with antibiotics. All parasite suspensions were stored at 4°C until required, up to a maximum storage time of 60 days.

3.2. Fluorescent microbeads

Dragon green-dyed polymer microspheres with a diameter of 1.90 ± 0.22 µm were obtained from Bangs Laboratories, Inc. (Fishers, IN). Beads were diluted into working solutions of distilled water with 0.1% Tween 20, and enumerated with a haemocytometer.

3.3. Microfluidic chip fabrication

The microfluidic structures of the chip were fabricated by the hot embossing of thermoplastic polymers using Epoxy replication moulds. The microchannel structure was initially transferred by standard photolithography to a Su-8 photoresist deposited on Si wafers that were used as master moulds. The Su-8 structures were transferred to a hard Epoxy mould (Conapoxy, CYTEX, USA) via an intermediate polydimethylsiloxane (PDMS) replica (mould inversion). These PDMS moulds were obtained by mixing PDMS (Sylgard 184, Dow Corning, USA) and curing agent at a 10:1 ratio and then degasing the mixture in a vacuum chamber for 30 min. The mixture obtained was poured onto the Su-8 mould and cured at 80^{o}C for 2 h. Similarly, the final Epoxy mould was obtained by pouring Epoxy resin mixed with curing agent (10:8 ratio) onto the intermediate PDMS mould and curing it at 120^{o}C for 6 h. The Epoxy moulds were then used to

emboss microfluidic features in thermoplastic elastomers (TPE) initially extruded from pellets into continuous films of 1.5 mm thickness. This embossing step was done with an EVG520 instrument (EV Group, Austria) operating at 135^{o}C and 6 kN of applied force for 5 min. The final chips were sealed by using plastic injected covers with integrated luer-lock ports. The injection machine used to fabricate these covers was an E110 Compression Injection Moulding System (Engel, USA). Due to its strong adhesion to the thermoplastic elastomeric films, a cyclo olefin polymer (Zeonor-Zeon Corporation, Japan) was used as material for the luer-lock covers in order to provide proper seal of the microfluidic structure as well as simple connectivity to the external syringe pumping system (Harvard Apparatus, USA). The fluidic connection between the microfluidic device and the pumping system was done with laboratory tubing (Dow Corning, USA) and standard luer-lock connectors (Qosina, USA). Advanced handling and sample recirculation through the chip is also done by using 3-way (T) luer-lock check valves (Qosina, USA).

3.4. Device characterization.

The microfluidic chips consisted of an inlet (I) port leading to the main separation channel (SC) which consists of a rectangular microfluidic channel. The separation channel enlarges into the large channel (LC), which splits into three smaller channels connected directly to three output ports (C, E1 and E2) (Fig. 6a and b). In the LC, flow is slowed down to allow enhanced visualization of fluorescent particles. The SC is 70 ± 2 μm wide and 180 ± 5 μm deep in the *Giardia* inertial separation chip and 40 ± 2 μm wide and 180 ± 5 μm deep in the *Cryptosporidium* inertial separation chip. The tolerances in these dimensions originate in a certain degree of imprecision that occurs in embossing replicas due to the thermal expansion of

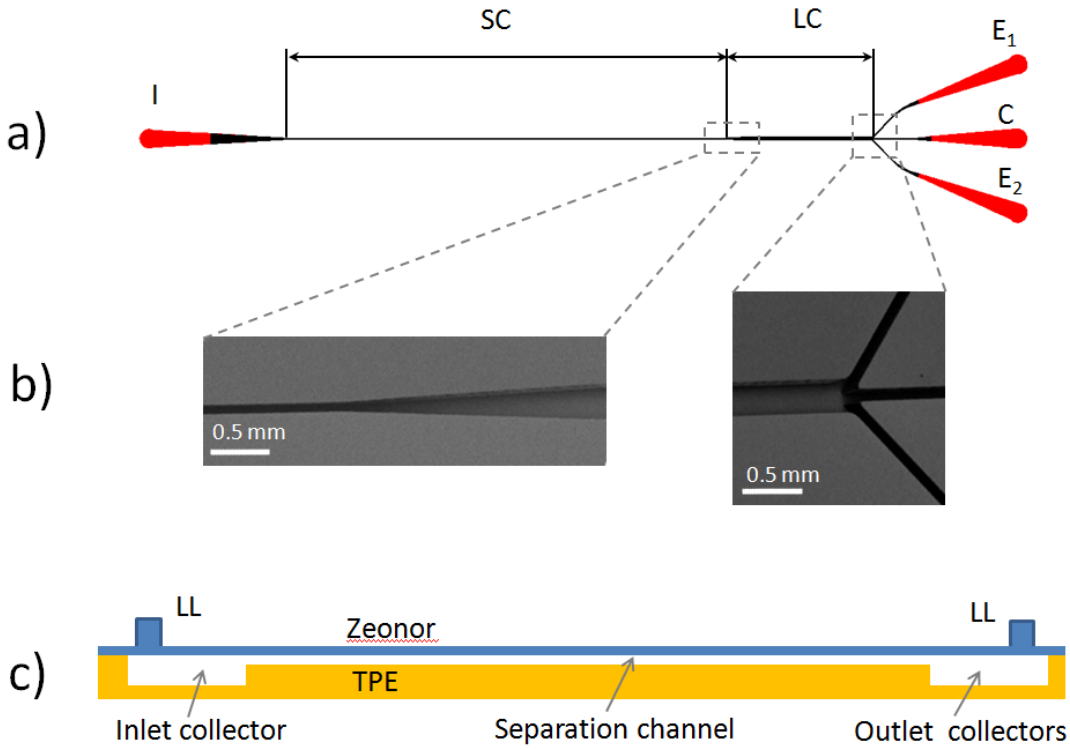
a)
SC
LC
I
E_1
C
E_2
b)
0.5 mm
0.5 mm
c)
LL
Zeonor
LL
TPE
Inlet collector
Separation channel
Outlet collectors

Fig. 6 Schematic representation and characterization of the microfluidic chip a) inlet (I) port allow entry into the separation channel (SC) which then widens into a large channel (LC) that splits into three outlet collectors (C, E1 and E2); b) Scanning electron microscopy images of the transition region from the separation channel to the observation window as well as the outlet trifurcation; c) schematic representation of a vertical section along the separation channel showing the Zeonor-TPE chip assembly with the luer-lock (LL) ports, separation channel and input and output collectors. The regions between the Zeonor cover and the TPE film qualitatively illustrate the depth of the embossed features.

the TPE itself, as well as to the mechanical stresses that are induced at the assembling step. The LC connecting the separation channel to the outlet trifurcation outlets is about 300 μm wide and is the same depth as the SC. The SC and the LC have lengths of 42 mm and 15 mm, respectively. All inlet and outlet collectors are 500 μm deep, which is much deeper than the SC or observation window (Fig. 6c) to avoid collapse of the relatively large TPE structures at the inlet and outlet ports.

3.5. Inertial separation chip setup and run procedures

An example of a microfluidic setup for the concentration of *G. duodenalis* cysts consisting of two syringe pumps, two reservoirs (waste and sample), a microfluidic concentration unit and four T check valves is given in Fig. 7a and b. The samples were initially loaded into a syringe (plastic pack 10 mL, Benson-Dickinson, USA) and mounted on a syringe pump (pump 1). The syringe is connected with a T valve to the chip inlet and to the sample/recovery reservoir. Similarly, three additional syringes are connected with T valves to the chip outlets and to the two reservoirs as indicated in the figure. The T valves are two-way valves which open on top (d1) when pushed by the syringe and open on the side (d2) when pulled by the syringe. The pumps are programmed to re-cycle the sample liquid through the microfluidic unit until the desired final concentration (target volume) is reached by using a specific protocol such as the ones for *G. duodenalis* in Table 1 or *Cryptosporidium* spp. in Table 2. As the main separation channel splits into three smaller channels of equal size, one third of the total volume being cycled through the chip is pumped into the waste reservoir, while two thirds of the total volume is cycled into the recovered reservoir, where it can be re-cycled through the system once more. As the components of the pumping system, including the chip, occupy roughly 1 ml of volume, prior to loading the sample, 1 ml of ddH_2O was loaded into the syringe on pump 1 and pumped into the system in order to prime the chip with fluid and prevent the circulation of air in the system. Total run time

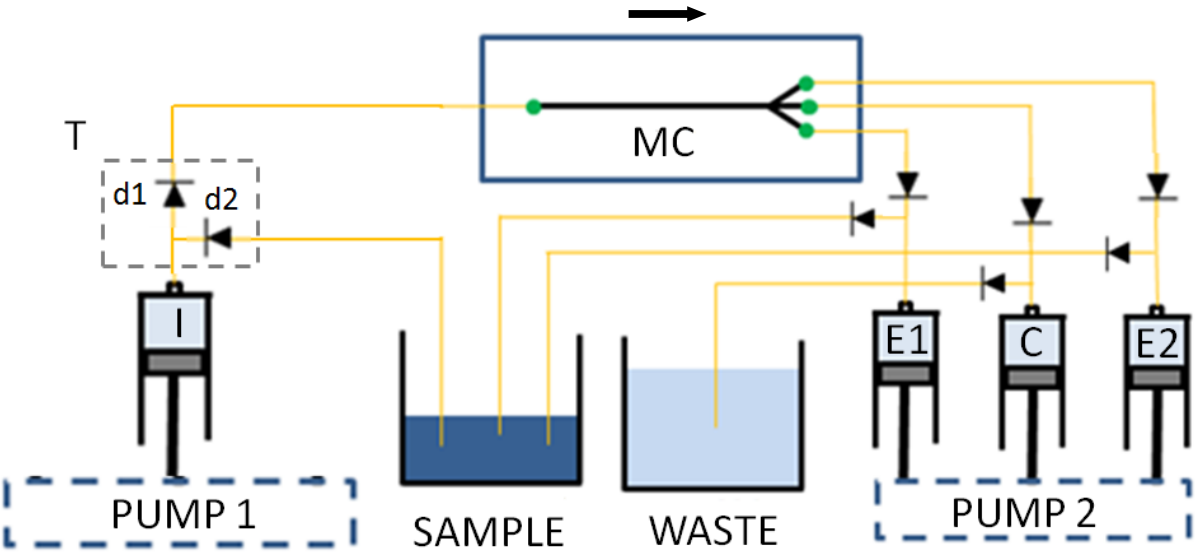
T
d1
d2
MC
I
E1
C
E2
PUMP 1
SAMPLE
WASTE
PUMP 2

A)

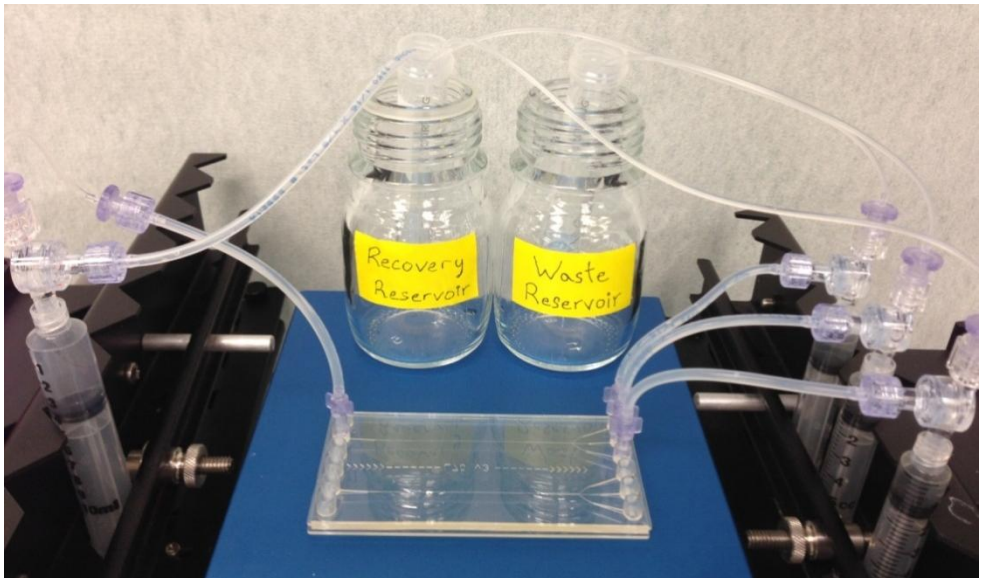
Recovery Reservoir
Waste Reservoir

B)

Fig. 7 Schematic representation (A) and actual image (B) of the fluidic setup used for the concentration of parasites with the microfluidic inertial separation chip (MC). The directional arrow at the top of the diagram represents the direction of flow through the chip. The T check valve on the inlet (I) syringe is open at d2 when the sample is pulled into the syringe. During the pumping of the solution out of the syringe and into the chip, d2 is closed and d1 is open.

Cycle #	Pump 1 Program	Pump 2 Program
1	Infuse 10.0 ml @ 1.2 ml/min Wait for 1.0 min Withdraw 6.667 ml at 6.667 ml/min	Withdraw 3.333 ml at 0.4 ml/min Infuse 3.333 ml at 3.333 ml/min Wait for 1.0 min
2	Infuse 6.667 ml @ 1.2 ml/min Wait for 0.667 min Withdraw 4.444 ml at 6.667 ml/min	Withdraw 2.222 ml at 0.4 ml/min Infuse 2.222 ml at 3.333 ml/min Wait for 0.667 min
3	Infuse 4.444 ml @ 1.2 ml/min Wait for 0.444 min Withdraw 2.963 ml at 6.667 ml/min	Withdraw 1.481 ml at 0.4 ml/min Infuse 1.481 ml at 3.333 ml/min Wait for 0.444 min
4	Infuse 2.963 ml @ 1.2 ml/min Wait for 0.296 min Withdraw 1.975 ml at 6.667 ml/min	Withdraw 0.988 ml at 0.4 ml/min Infuse 0.988 ml at 3.333 ml/min Wait for 0.296 min
5	Infuse 1.975 ml @ 1.2 ml/min Wait for 0.198 min Withdraw 1.317 ml at 6.667 ml/min	Withdraw 0.658 ml at 0.4 ml/min Infuse 0.658 ml at 3.333 ml/min Wait for 0.198 min
6	Infuse 1.317 ml @ 1.2 ml/min	Withdraw 0.439 ml at 0.4 ml/min Infuse 0.439 ml at 3.333 ml/min

TABLE 1. *Giardia duodenalis* cyst pumping protocol for the concentration of a 10 ml sample with the *Giardia* microfluidic inertial separation chip.

Cycle #	Pump 1 Program	Pump 2 Program
1	Infuse 10.0 ml @ 0.4 ml/min Wait for 75 sec Withdraw 6.667 ml at 5.333 ml/min	Withdraw 3.333 ml at 0.133 ml/min Infuse 3.333 ml at 2.667 ml/min Wait for 75 sec
2	Infuse 6.667 ml @ 0.4 ml/min Wait for 50 sec Withdraw 4.444 ml at 5.333 ml/min	Withdraw 2.222 ml at 0.133 ml/min Infuse 2.222 ml at 2.667 ml/min Wait for 50 sec
3	Infuse 4.444 ml @ 0.4 ml/min Wait for 33.33 sec Withdraw 2.963 ml at 5.333 ml/min	Withdraw 1.481 ml at 0.133 ml/min Infuse 1.481 ml at 2.667 ml/min Wait for 33.33 sec
4	Infuse 2.963 ml @ 0.4 ml/min Wait for 22.22 sec Withdraw 1.975 ml at 5.333 ml/min	Withdraw 0.988 ml at 0.133 ml/min Infuse 0.988 ml at 2.667 ml/min Wait for 22.22 sec
5	Infuse 1.975 ml @ 0.4 ml/min Wait for 14.82 sec Withdraw 1.317 ml at 5.333 ml/min	Withdraw 0.658 ml at 0.133 ml/min Infuse 0.658 ml at 2.667 ml/min Wait for 14.82 sec
6	Infuse 1.317 ml @ 0.4 ml/min	Withdraw 0.439 ml at 0.133 ml/min Infuse 0.439 ml at 2.667 ml/min

TABLE 2. *Cryptosporidium* spp. oocyst pumping protocol for the concentration of a 10 ml sample with the *Cryptosporidium* microfluidic inertial separation chip.

for the six cycle *Giardia* concentration protocol represented in Table 1 is 28 min, 17 sec (Fig. 8) and 75 min, 15 sec for the *Cryptosporidium* concentration protocol represented in Table 2. Any liquid remaining in the chip at the end of the run was withdrawn using pump 2 and pumped into the respective reservoirs. The suspensions in both the waste and sample/recovery reservoirs were collected for analysis.

3.6. Concentration of (oo)cysts in pure suspension

Approximately 1,000 *G. duodenalis* cysts or *C. parvum* oocysts were isolated by serial dilution of the stock 1.25 x 10^6 (oo)cyst per ml suspension in 1X PBS. The (oo)cysts were then added to 10 ml of elution buffer containing 1X PBS and 0.01% Tween-80, pH 7.4. The 10 ml sample was vortexed thoroughly, loaded into a 10 ml syringe and cycled through the inertial microfluidic separation chip as described in Table 1. The final suspensions pumped into the recovered reservoir (approximately 1.5 ml) and waste reservoir (approximately 9.5 ml), at the end of the run, were centrifuged at 3,724 x g for 15 min. The supernatant was removed, leaving each sample with a final suspension of approximately 500 µl. The efficiency of the inertial separation chips in concentrating (oo)cysts from buffer was determined by enumerating a portion of the initial inoculum, the final concentrate suspension, and the waste suspension. The enumeration was performed by epifluorescence microscopy as described below.

3.7. Separation of (oo)cysts from fluorescent beads

A 2.653 x 10^9 per ml stock solution of microbeads was serially diluted down to approximately 6 x 10^3 in 1X PBS. These 1.90 µm fluorescent beads along with either 2,000 *G. duodenalis* cysts or 2,000 *C. parvum* oocysts, were spiked into 10 ml of elution buffer containing 1X PBS and 0.01% Tween-80, pH 7.4. The 10 ml sample was vortexed thoroughly, loaded into a 10 ml syringe and cycled through the inertial separation chip for either one, three or six cycles. The final

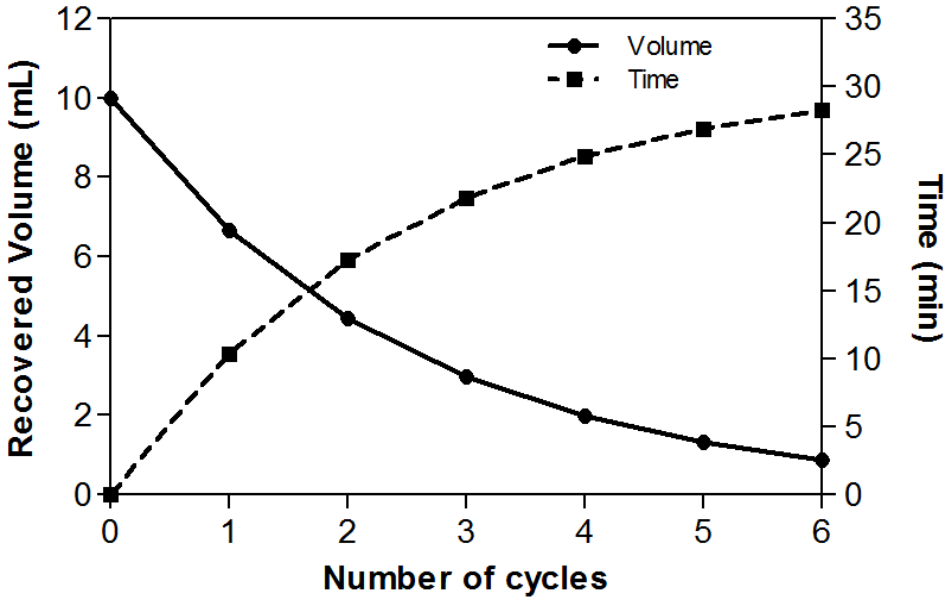
Volume
Time
Recovered Volume (mL)
Time (min)
Number of cycles
0
2
4
6
8
10
12
0
5
10
15
20
25
30
35
0
1
2
3
4
5
6

Fig. 8 Concentration of a 10 ml suspension with the *Giardia* inertial separation chip. Theoretical volume cycled into the recovered reservoir over 0-6 cycles using a working flow rate of 1.2 ml/min and the associated run times.

concentrated parasite suspension of approximately 1.5 ml, and the approximately 9.5 ml of waste solution were centrifuged at 3,724 x g for 15 min. The supernatant was removed leaving each sample with a final suspension of approximately 500 µl. The efficiency of the inertial separation chip in separating out non-specific microparticles and concentrating (oo)cysts over a range of cycles was determined by enumerating a portion of the final concentrate suspension and the waste suspension. The enumeration was performed by epifluorescence microscopy as described below.

3.8. Enumeration by epifluorescence microscopy

A 100 µl aliquot of the final 500 µl sample was incubated with Crypto/Giardia Cel Reagent FITC-labeled monoclonal antibodies (Cellabs, Brookvale, Australia) for 1 h at room temperature. The suspension was rinsed of any unbound antibodies by diluting in 1 ml of PBS. The sample was centrifuged once more and the supernatant was aspirated off leaving the labeled parasites in 100 µl of solution. Twenty microliter aliquots of the resuspended suspension were pipetted onto microscope slides (Fisher Scientific, Pittsburgh, PA). The (oo)cysts and/or fluorescent microbeads observed on each of three slides were enumerated on a Nikon 80i epifluorescence microscope (Nikon Canada, Inc., Mississauga, ON) at 200 X magnification, using a blue filter with excitation at 450 to 490 nm. The total number of (oo)cysts and/or fluorescent microbeads on the three slides were added and multiplied by the appropriate factor to obtain the total number per sample.

3.9. Preparation of artificially contaminated food samples

Pre-packaged salad kits were purchased at retail. The contents of these kits were pre-chopped and pre-washed by the manufacturer. Salad kits were stored at 4°C and used prior to their expiration dates. Twenty five (±0.5) gram samples of Romaine lettuce, taken from the salad kits,

were weighed out in Stomacher™ bags (Seward, Worthing, UK). Purchased *G. duodenalis* cyst suspensions were diluted in ddH_2O to obtain an initial suspension with a concentration of approximately 300 cysts per 750 µl. Six 2-fold serial dilutions of the 300 cyst parasite suspension were performed. Each of the six dilutions was used to inoculate duplicate lettuce samples. Each lettuce sample was spiked with 750 µl of the parasite suspension and added drop-wise to the surface of the lettuce leaves in each Stomacher™ bag. Two additional lettuce samples were inoculated with 750 µl of ddH_2O and used as negative controls. Samples were air dried at room temperature for 2 h, then refrigerated at 4°C overnight prior to analysis.

3.10. Inertial separation method for the elution and concentration of cysts from lettuce

Twenty five gram lettuce samples were submerged in 200 ml of elution buffer containing 1X PBS and 0.01% Tween-80, pH 7.4, in a stomacher bag. Samples were agitated on an orbital shaker at 120 rpm for 15 min. The contents of the bag were then vacuum-filtered through a sheet of polyester monofilament with a 10 µm pore size (IFC fabrics, Minneapolis, MN) to remove any large particles. The filtered suspension was then centrifuged at 2,000 x g for 15 min at 4°C. A total of 190 ml of supernatant was removed, leaving a final concentrated suspension of 10 ml. The 10 ml suspension was vortexed thoroughly, loaded into a 10 ml syringe and cycled through an inertial microfluidic separation chip for six cycles as described in Table 1. The final collected suspension of approximately 2 ml was centrifuged at 1,500 x g for 10 min, and the supernatant was removed leaving a final suspension of approximately 500 µl.

3.11. Conventional method for the elution and concentration of cysts from lettuce

G. duodenalis cysts were eluted from the spiked lettuce and initially concentrated according to the method of Dixon et al. (17), which is specific for the detection of *Cyclospora*, *Cryptosporidium*, and *Giardia* from ready-to-eat packaged leafy greens. In brief, the method

involved weighing 25 g samples into 1 L capacity Stomacher™ bags and adding 200 ml of elution buffer containing 1X PBS and 0.01% Tween-80, pH 7.4. Bags were next placed on an orbital shaker for 15 min at 120 rpm. The elution buffer was then poured into centrifuge tubes through four layers of gauze within a funnel to trap larger particles. Particles in the elution buffer were concentrated by a series of centrifugation steps at 2,000 x g for 15 min at 4°C, followed by removal of the supernatant. The remaining suspension containing the pellet of cysts and background particles was transferred to a 1.5 ml microcentrifuge tube and brought to a final volume of 500 µl with elution buffer.

3.12. Limit of detection and percent recovery of *G. duodenalis* cysts

The limit of detection (LOD) and percent recovery of cysts was assessed on lettuce samples artificially-contaminated with *G. duodenalis* cysts (described above) for both the inertial separation method and a conventional method used by Dixon et al. (17), which was considered the gold standard. Of the 14 total samples in each trial, half were eluted and concentrated using the inertial separation method, while the second half were eluted and concentrated in parallel using the conventional method of Dixon et al. (17). Each sample was screened for the presence of *G. duodenalis* cysts by epifluorescence microscopy as described above. Three slides making up 60 µl of the final sample were examined. The percent recovery was determined by enumerating a portion of the initial inoculum, and the concentrate recovered from the samples spiked with the highest inoculum as described above. The LOD and percent recovery was determined by three replicate experiments.

3.13. Particle enumeration of final concentrate by flow cytometry

A 50 µl portion of the remaining recovered parasite suspension was analyzed by flow cytometry in order to estimate the efficiency of the inertial separation method in removing background

lettuce/food particles. The sample was stained with Crypto/Giardia Cel Reagent, diluted in 200 µl of PBS, and 10 µl of Absolute Count Standard Beads (Bangs Laboratories, Fisher, IN) was added. The Absolute Count Standard Beads were used to ensure that equal portions of each sample were analyzed. Sample analyses were performed using a Becton Dickinson FACS Calibur equipped with a 488 nm air-cooled laser (BD Biosciences, Mississauga, ON). The total number of background particles (events) per sample was determined by subtracting the number of *G. duodenalis* cyst events and bead events detected, from the total number of events detected by the cytometer. The average proportion of background particles in the final concentrated parasite suspension for both the inertial microfluidic method and the conventional method were compared and used to estimate the purity of the parasite suspensions.

3.14 Statistical analysis

Comparative analysis was performed using the Mann-Whitney non-parametric test to determine if there was a significant difference among the cyst percent recoveries. A level of significance of 5% ($\alpha = 0.05$) was used to test for statistical differences. Analysis was done using GraphPad Prism 5, version 5.03 (GraphPad Software, Inc).

4.0 RESULTS

4.1 Specificity and concentration efficiency of the inertial separation chips for (oo)cysts suspended in buffer

The specificity of the third version of the *Giardia* inertial separation chip for *G. duodenalis* cysts suspended in 10 ml of 1X PBS and 0.01% Tween-80 elution buffer and the efficiency of concentration was initially assessed to determine the ability of the chip to focus cysts from a relatively particle free cyst suspension. A 20-fold concentration was achieved, with 72.44 ± 1.77% (n=3) of *G. duodenalis* cysts recovered (Fig. 9). An average of 16.49 ± 5.40% (n=3) of *G. duodenalis* cysts were not focused towards the outside of the channel and were, thus, cycled out of the chip into the waste reservoir. There was also an average of 11.07 ± 7.14% (n=3) of *G. duodenalis* cysts that were lost to the components of the system (i.e., channels, valves, tubing or syringes).

Initial experiments with the first version of the *Cryptosporidium* inertial microfluidic separation chip (Fig. 10) once more involved the concentration of *C. parvum* oocysts suspended in 10 ml of 1X PBS and 0.01% Tween-80 elution buffer. These experiments, however, were not as successful as the initial experiments with the *Giardia* inertial separation chip. The recovery of oocysts in the final concentrate suspension was much lower with an average of 45.87 ± 8.36% (n=3). This was primarily attributed to the loss of sample due to leaking at the input and output connector sites of the microfluidic chip. The leaking occurred with the *Cryptosporidium* inertial separation microfluidic chip and not the *Giardia* inertial separation microfluidic chip, because the dimensions of the *Cryptosporidium* separation channel were much smaller, which lead to increased pressures within the chip. In addition, the smaller channel required the slower working flow rate of 0.6 ml/min versus the 1.2 ml/min required for the *Giardia* inertial

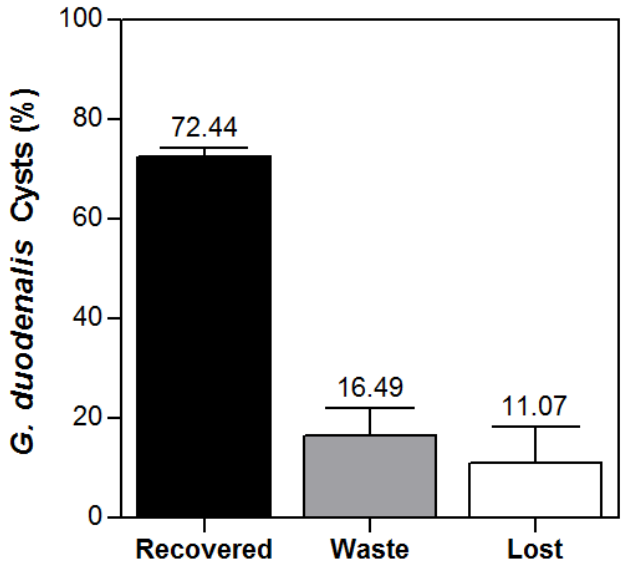
100
80
60
40
20
0
G. duodenalis Cysts (%)
72.44
16.49
11.07
Recovered
Waste
Lost

Fig. 9 *Giardia duodenalis* cysts recovered from 10 ml of spiked buffer following concentration with the *Giardia* inertial separation chip. A portion of the spike, recovered concentrate and waste suspension cycled out of the chip, was stained with Crypto/Giardia Cel Reagent FITC-labeled monoclonal antibodies and excited at 450 to 490 nm for enumeration by immunofluorescence microscopy. The cysts that were not found in the recovered or waste suspensions were deemed as experimental loss. Error bars represent SD from three separate experiments.

Fig. 10 Version 1 of the inertial separation microfluidic chip. Top down image of the *Cryptsoporidium* inertial separation chip which is also representative of the *Giardia* inertial separation chip. The microchannel is hot-embossed into the top of the bottom polymer wafer and the channel is sealed with a hard plastic cover. Inlet and outlet ports consisting of metal tubes leading to the inlet and outlet collectors of the separation channel are attached and sealed with epoxy following fabrication.

separation chip to reach the ideal transfer flow rate of 10 ml/min. Even with the slow working flow rate, it appeared that the pressure inside the *Cryptosporidium* microfluidic chip was greater than the *Giardia* microfluidic chip. The greater pressure within the chip most likely caused the leaking at the initial inlet and outlet ports which in the first version of the chip (Fig. 10), consisted of metal tubes sealed with epoxy. This problem was targeted in the design of the second version of the chip (Fig. 11), which contained a number of design and fabrication improvements including the addition of integrated luer-lock connectors (Fig. 6C). The luer-lock connectors greatly reduced the amount of leakage; however, there was the occasional run where leaking still occurred. This issue was addressed once more by reducing the working flow rate from 0.6 ml/min to 0.4 ml/min. This in turn resulted in a reduction of the ideal transfer flow rate within the channel to drop from 10 ml/min to 8 ml/min, however, this transfer flow rate still seemed to provide efficient focusing of the oocysts. Using the new version of the microfluidic chip and a slower flow rate, a 20- fold concentration of *C. parvum* oocysts in buffer achieved recoveries of 68.57 ± 12.98% (n=3) (Fig. 12). An average of 25.35 ± 3.68% (n=3) of oocysts were cycled out of the chip into the waste reservoir, and 6.08 ± 4.08% (n=3) cysts were lost during the procedure.

4.2 Efficiency of the inertial separation chips in separating out non-specific microparticles

To i) further investigate the *G. duodenalis* cysts and *C. parvum* oocysts that were being lost in the waste reservoir, ii) determine the efficiency of the chips in cycling out non-specific microparticles, and iii) ultimately determine an optimal cycling number for use with food samples, 10 ml buffer suspensions containing *G. duodenalis* cysts or *C. parvum* oocysts and non-specific microparticles (beads) with a mean diameter of 1.90 µm were pumped through their respective microfluidic inertial separation chips for one, three and six cycle protocols. The small bead particles are similar in size to some lettuce/food particles which may be inhibitory to

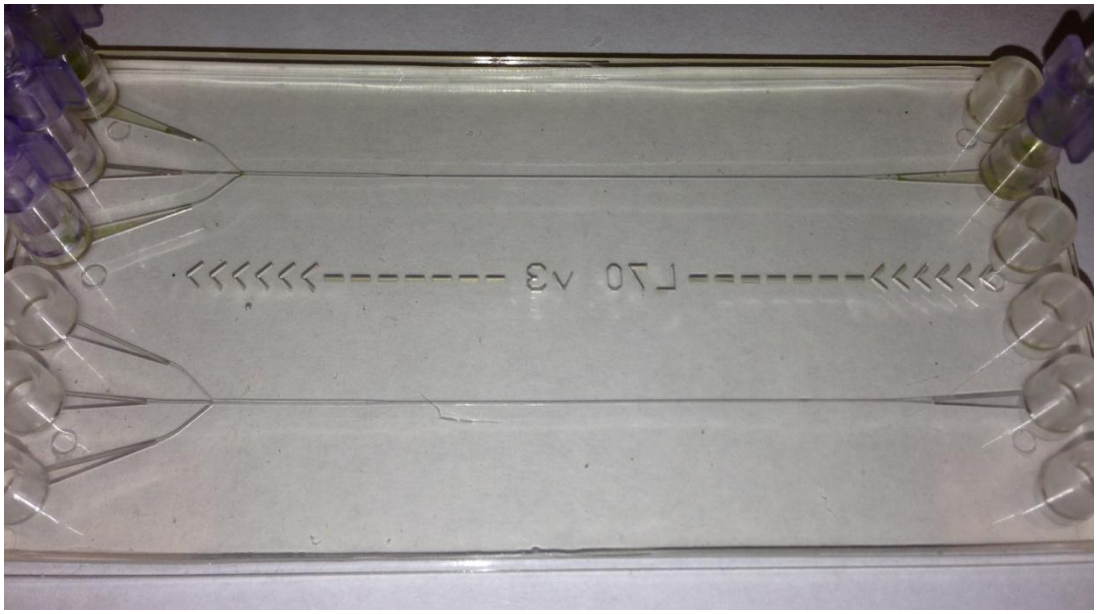

Fig. 11 Version 2 of the inertial separation microfluidic chip. The inlet and outlet ports consist of luer-locks that are integrated into the chips during the fabrication process and allow for simple connectivity to the external tubing leading to the syringe pumps. Each microfluidics chip also contains an additional inertial separation channel per chip that allows for processing a larger volume of sample or multiple samples to be run simultaneously.

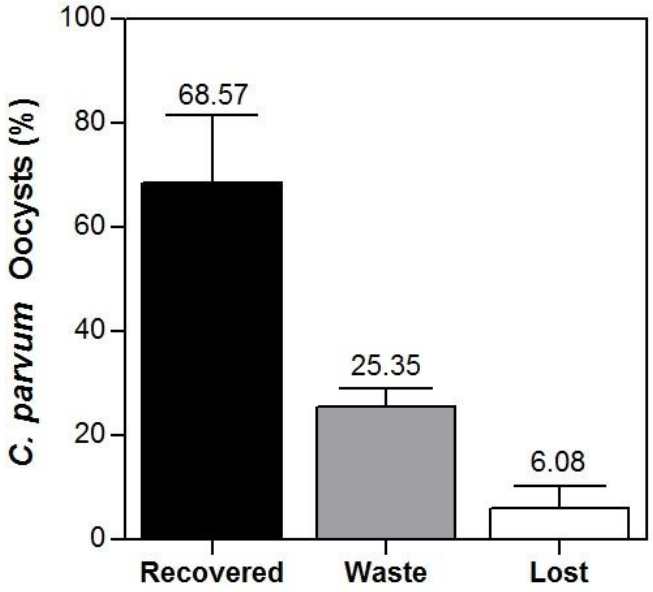
100
80
60
40
20
0
C. parvum Oocysts (%)
68.57
25.35
6.08
Recovered
Waste
Lost

Fig. 12 *Cryptosporidium parvum* oocysts recovered from 10 ml of spiked elution buffer following concentration with the *Cryptosporidium* inertial separation chip. A portion of the spike, recovered concentrate and waste suspension cycled out of the chip, was stained with Crypto/Giardia Cel Reagent FITC-labeled monoclonal antibodies and excited at 450 to 490 nm for enumeration by immunofluorescence microscopy. The oocysts that were not found in the recovered or waste suspensions were deemed as experimental loss. Error bars represent SD from two separate experiments.

detection methods and were not expected to focus towards the channel walls, and were thus expected to be separated out into the waste reservoir during the cyclic concentration process. Suspensions from the recovered and waste reservoirs were collected and enumerated following one, three and six cycles of focusing. The proportions of cysts in each of the reservoirs were compared. Following one cycle, 92.14 ± 3.93% (n=2) of the *G. duodenalis* cysts were found in the recovered reservoir, 87.47 ± 5.53% (n=2) following three cycles, and 81.93 ± 7.87% (n=2) following six cycles (Fig. 13). Thus, initially during the first cycle, it appears that there is a greater rate of loss of the cysts, with 7.86% being found in the waste reservoir. This may be attributed to unfocused cysts that were outliers in terms of size, or to cysts clumping together and becoming larger particles. Over one to six cycles it appears that there was a constant rate of loss of 2.04% cysts per cycle, which is much lower than the loss observed over the first cycle. A similar pattern of loss was seen with the *Cryptosporidium* inertial microfluidic separation. Following one cycle, 91.51 ± 2.25% (n=2) of the *C. parvum* oocysts were found in the recovered reservoir, 84.61 ± 0.40% (n=2) following three cycles, and 74.54 ± 5.31% (n=2) following a 6 cycle run (Fig. 14). Thus as with the *Giardia* inertial separation, there was an initial large loss of 8.49% of oocysts following 1 cycle followed by a constant rate of loss of 3.45% oocysts per cycle.

With respect to the fluorescent beads, following a one cycle *Giardia* inertial microfluidic separation run, 54.96 ± 14.88% (n=2) of the beads were found in the recovered reservoir, 45.11 ± 10.69% (n=2) following three cycles, and 29.52 ± 3.17% (n=2) following six cycles (Fig. 13). Thus, as expected, cycling the recovered suspension through the chip additional times helped to eliminate more non-specific microparticles from the recovered parasite suspension. As seen with the cysts, it appears that initially there is a large elimination of beads (45.04%) during the first

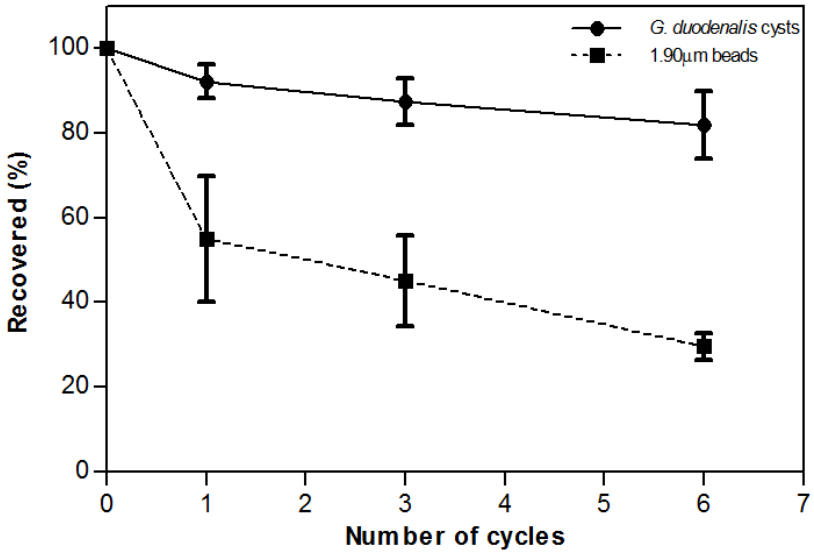
G. duodenalis cysts
1.90µm beads
Recovered (%)
100
80
60
40
20
0
0
1
2
3
4
5
6
7
Number of cycles

Fig. 13 Specificity of the *Giardia* inertial microfluidic separation chip for *G. duodenalis* cysts. The proportion of *Giardia duodenalis* cysts and green-dyed polymer microbeads in the recovered concentrate following one, three and six cycles of inertial separation. Portions of the recovered and waste suspensions were stained with Crypto/Giardia Cel Reagent FITC-labeled monoclonal antibodies and excited at 450 to 490 nm for enumeration by immunofluorescence microscopy. Error bars represent SD from two separate experiments.

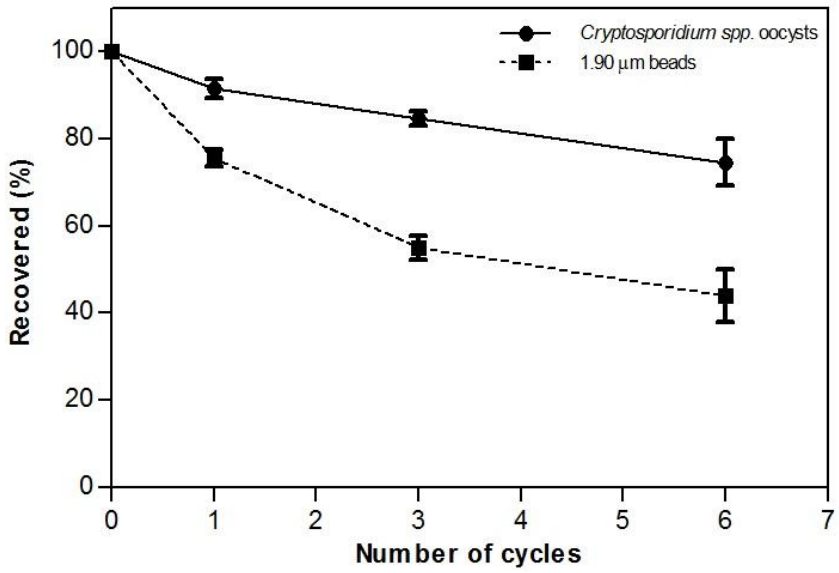
Cryptosporidium spp. oocysts
1.90 µm beads
Recovered (%)
100
80
60
40
20
0
0
1
2
3
4
5
6
7
Number of cycles

Fig. 14 Specificity of the *Cryptosporidium* inertial microfluidic separation chip for *C. parvum* oocysts. The proportion of *Crptosporidium parvum* oocysts and green-dyed polymer microbeads in the recovered concentrate following one, three and six cycles of inertial separation. Portions of the recovered and waste suspensions were stained with Crypto/Giardia Cel Reagent FITC-labeled monoclonal antibodies and excited at 450 to 490 nm for enumeration by immunofluorescence microscopy. Error bars represent SD from two separate experiments.

cycle, followed by a constant rate of elimination of 5.09% of beads per cycle over the remaining cycles. Following a one cycle *Cryptosporidium* inertial microfluidic separation run, 75.57 ± 2.05% (n=2) of the 1.90 µm beads were found in the recovered reservoir, 55.00 ± 2.80 (n=2) following three cycles, and 43.98 ± 6.03% (n=2) following six cycles (Fig. 14). Unlike with the *Giardia* inertial separation, it appears that the rate of loss of beads was not constant and slowed as the cycle number increased, just as the volume of suspension being pumped into the waste reservoir slowed. Thus, a greater proportion of the fluorescent beads were eliminated at every cycle in the *Giardia* inertial microfluidic separation run as compared to the *Cryptosporidium* inertial microfluidic separation.

4.3 Concentration and separation of *G. duodenalis* cysts recovered from spiked lettuce samples using an inertial separation integrated method

To directly assess the potential of microfluidic inertial separation chips as a concentration and filtration device in food microbiological analyses, the *Giardia* inertial separation chip was incorporated into a method for the recovery and detection of *G. duodenalis* cysts from lettuce. Due to its initial success in concentrating *G. duodenalis* cysts and eliminating non-specific particles, the *Giardia* inertial separation chip along with the six cycle concentration protocol was incorporated into an existing conventional method. Integrating the chip into the existing conventional method for the elution, separation and concentration of *G. duodenalis* from lettuce samples proved to be difficult. Initial experiments enumerating the recovered cysts in the final parasite samples, demonstrate a number of large lettuce particles (Fig. 15A). Thus, a number of large food particles must not have been separated out from the 200 ml eluent during filtration through layers of gauze, as required by the conventional method. The large food particles found in the recovered concentrate were as large as 1 mm, and thus had the potential to block the much

A **B**

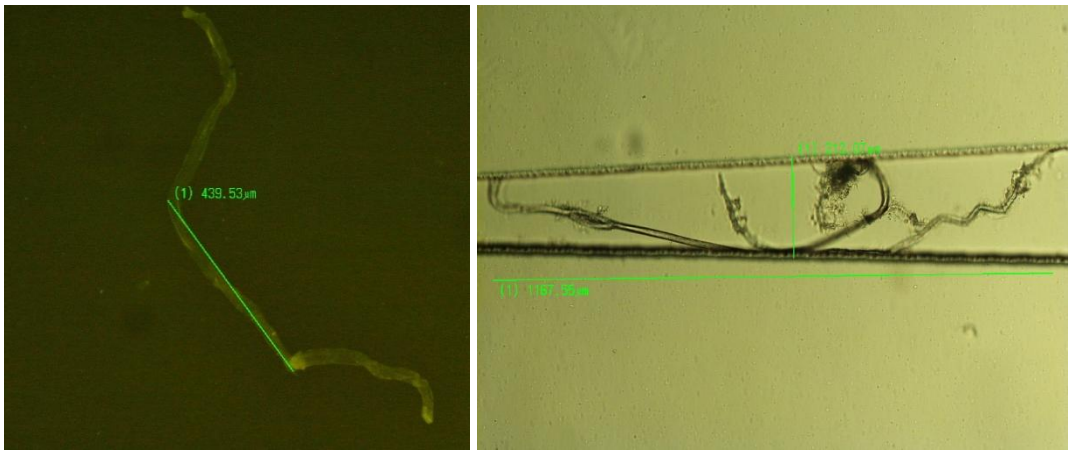

Fig. 15 Large food particles still present in the eluted parasite suspension following conventional filtration may impede inertial separation. Microscopic image at 100× magnification under blue (450-490 nm) light of auto-fluorescing food particles found in the final parasite concentrate (A) and of food particles partially blocking the inertial separation channel of a microfluidic chip under bright field (B).

smaller 70 µm wide *Giardia* separation channel (Fig. 15B) and/or affect the flow rate within the channel, which could lead to cysts not being focused or cysts being trapped within the microfluidic chip, which would ultimately lead to lower percent recoveries. To resolve these potential issues, the filtration of the initial 200 ml lettuce and parasite suspension eluted from the lettuce samples was addressed. Filtration methods using polyester monofilament filters with either 10 µm (Fig. 16A) or 35 µm openings (Fig.16B), under vacuum or gravity filtration, were compared to each other, as well as to the conventional gauze filtration method. The percent recovery of *G. duodenalis* cysts following elution, filtration by one of the five methods, and inertial separation were compared. It was found that the highest average percent recovery was obtained by using the filter with 10 µm openings (Fig. 16A) under vacuum. This filtration method was thus integrated into the inertial separation method.

Following optimisation, the effectiveness of this new method incorporating inertial microfluidic separation, was assessed against the conventional method of Dixon et al. (17). The effectiveness of the inertial separation method for use on lettuce samples artificially contaminated with *G. duodenalis* cysts was assessed by comparing the LOD and percent recovery of the two methods, and comparing the number of background particles in the final suspensions. The LOD of the inertial separation method for *G. duodenalis* cysts in spiked lettuce samples was 38 cysts per 25g sample. As shown in Table 3, the method enabled the identification of a minimum of one *G. duodenalis* cyst in each of the samples spiked with 38 cysts or more in each of the three trials, while the samples spiked with 19 or less were negative in each trial. The conventional method (17) enabled the identification of at least one *G. duodenalis* cyst in the samples spiked with 19 cysts or more for each of the three trials. The conventional method, however, did not yield any positive results for the samples spiked with

A **B**

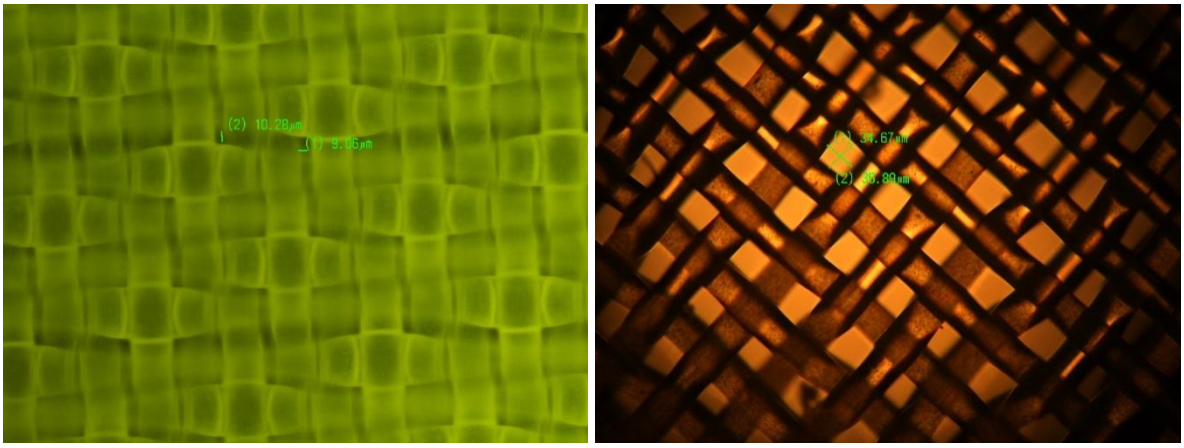

Fig. 16 Polyester monofilament filters removed large food particles and improved inertial focusing of (oo)cysts. Microscopic images at 200× magnification of the 10 μm pores of the PES 10 filter (A) and the larger 35 μm pores of the PES 20 filter (B). Filters were examined under visible light at various ends of the spectrum to provide contrast.

G. duodenalis cysts		Positive samples per trial	
Per 25 g lettuce sample	Expected in proportion analyzed[b]	Microfluidic method	Conventional method
300 (225-425)[a]	36	3/3	3/3
150	18	3/3	3/3
75	9	3/3	3/3
38	5	3/3	3/3
19	2	0/3	3/3
9	1	0/3	0/3

[a] Range of cysts for samples spiked with the highest dilution in three trials. Actual average of three trials was 296 cysts.
[b] Theoretical total number of possible *G. duodenalis* cysts present on the three 20 µl slides analyzed from the total 500 µl final concentrate.

TABLE 3 Limit of detection of *Giardia duodenalis* cysts artificially-inoculated on lettuce samples; based on the number of positive samples in three trials at each concentration.

only 9 cysts. Thus, the conventional method (17) had a slightly higher sensitivity. Parasites were not detected in any of the negative control samples that were spiked with ddH_2O. It may be possible to lower these detection limits even further by analyzing a larger proportion of the total sample volume (i.e., >60 µl of the total 500 µl sample). However, as immunofluorescence detection is very time-consuming, analyzing larger volumes of samples would likely not be efficient or cost-effective for routine laboratory testing.

The average percent recoveries of each method was determined by enumerating the number of cysts recovered in the final sample and the number of cysts in the spike used to inoculate the lettuce samples. The lettuce samples spiked with the highest concentration of *G. duodenalis* cysts in each trial of the LOD experiment were used to calculate the percent recoveries. The inertial separation method recovered an average of 68.39 ± 20.67% (n=3) of cysts in three trials, while the conventional method (17) recovered 80.00 ± 8.16% (n=3). The slightly lower percent recovery of cysts from the inertial separation method supports the slightly higher LOD. The results of the statistical test demonstrated that the mean percent recoveries obtained from the conventional method was not significantly higher ($P = 0.35$). Initial experiments with buffered cyst suspensions demonstrated that 11.07% of the cysts are lost in the chip and pumping system itself (Fig. 9), while another 16.49% is lost during the 6 cycle concentration process. The additional loss in recovery from the expected 72.44% obtained with buffered suspensions, down to 68.39%, can be attributed to the loss of cysts from the elution, vacuum filtration, or initial centrifugation steps of the method.

4.4 Particle enumeration of final concentrate

To determine the concentration of food particles and related debris in the final recovered concentrate, flow cytometry was performed on samples in each of the three trials which were

processed by either the conventional or inertial separation methods. The concentration of food particles and debris in each sample was correlated with the total number of background particles (events) analyzed by the cytometer. An approximately 10-fold decrease in background particles was observed in the lettuce samples that underwent the inertial separation method versus the conventional method (Fig. 17). The 10-fold reduction in background particles determined by flow cytometry suggested that the inertial separation method of analysis greatly reduces the concentration of food debris in the final sample.

The representative microscopic images in Fig. 18 qualitatively illustrate the additional difficulty background particles posed in the detection of fluorescently-tagged *G. duodenalis* cysts. The samples processed with the conventional method (Figs. 18*a* and 18*c*) contained a number of larger particles (>10 μm in diameter), which fluoresced red, green and yellow under blue light. These fluorescent background particles, were present at high concentrations, and could mask fluorescing *G. duodenalis* cysts, preventing their detection and leading to an increase in false-negative results. The samples processed by the conventional method also contained a number of smaller particles (≤10 μm in diameter) which non-specifically fluoresced and could be mistakenly identified as *G. duodenalis* cysts (6-10 μm) if analysis was not thorough, leading to the possibility of an increase in false-positive results. In comparison, the samples processed by the inertial separation method (Figs. 18*b* and 18*d*) had much fewer background fluorescent particles. This allowed for a greater ease and speed of detection of cysts during the LOD and enumeration assays, and reduced the probability of false-negative and false-positive results. These observations made by immunofluorescence microscopy support the quantitative results obtained by flow cytometry.

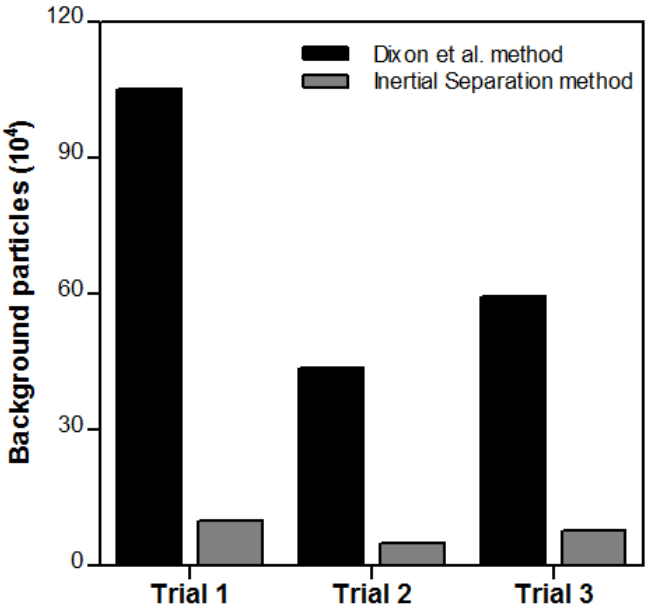
120
90
60
30
0
Background particles (10^4)
Dixon et al. method
Inertial Separation method
Trial 1
Trial 2
Trial 3

Fig. 17 10-fold reduction in background particles in the samples recovered from the inertial separation method. Fifty µl sub-samples of the recovered concentrate from the inertial separation and conventional method were analyzed by flow cytometry. Flow count standard beads ensured that equal proportions of the samples were analyzed by the cytometer. A background particle was defined as any event analyzed by the cytometer that was not a *Giardia duodenalis* cyst or a flow count bead.

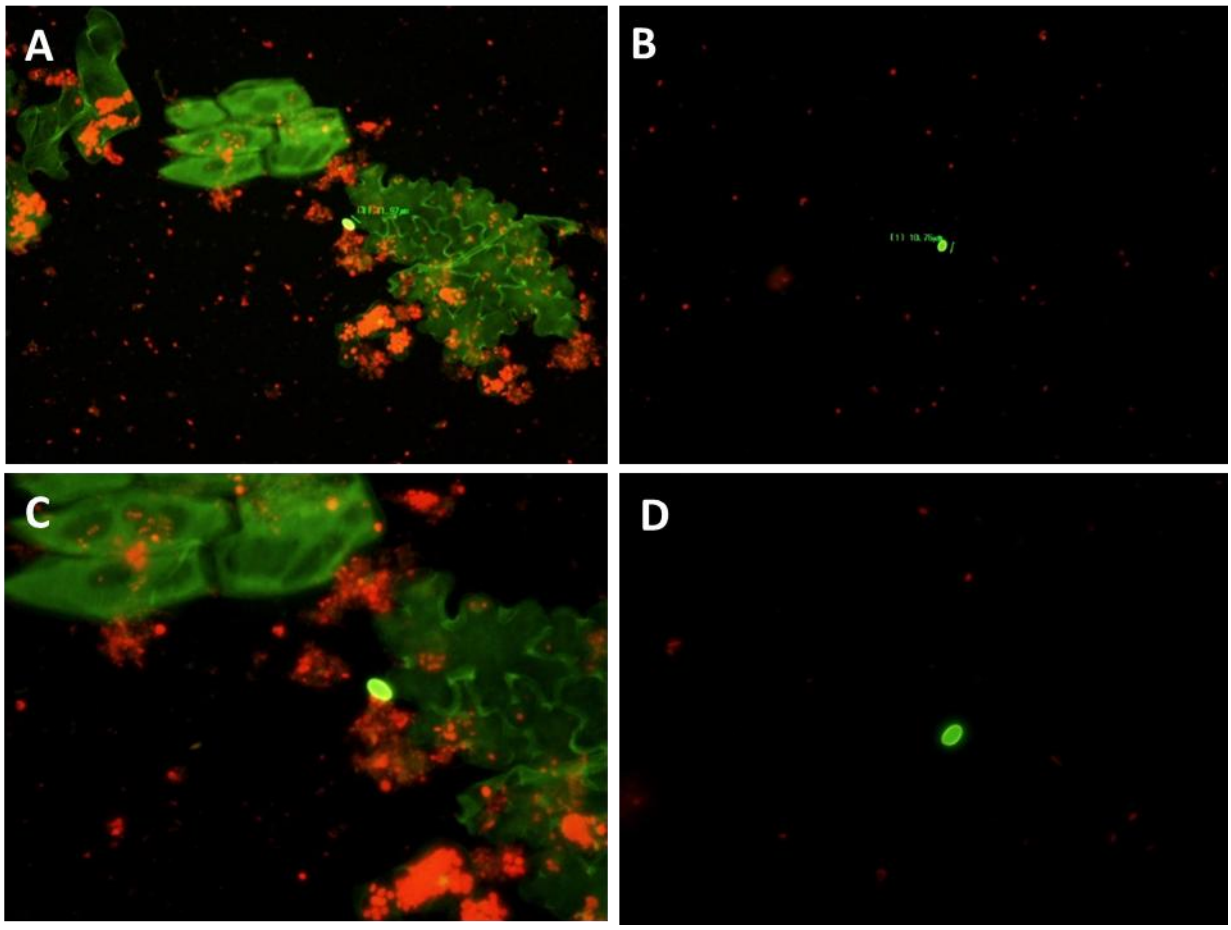
A
B
C
D

Fig. 18 Non-specific immunofluorescent emissions from lettuce particles impede *Giardia duodenalis* cyst detection. Representative microscopic images of the recovered concentrate from the conventional method at 200× (A) and 400× (C) magnification, and from the inertial separation method at 200× (B) and 400× (D) magnification. All samples were stained with Crypto/Giardia Cel Reagent FITC-labeled monoclonal antibodies and excited at 450 to 490 nm. Green bars adjacent to the *Giardia duodenalis* cyst in (A) and (B) are 11.97 µm and 10.76 µm in length respectively.

5.0 DISCUSSION

5.1 Specificity and efficiency of the inertial separation chips

The six cycle microfluidics concentration protocol is designed to eliminate approximately 9 ml (90%) of the initial 10 ml volume into the waste reservoir. Therefore, assuming homogeneity, if focusing by inertial separation was not occurring, approximately 90% of the (oo)cysts would be expected in the waste reservoir, and 10% in the recovered reservoir. The *Giardia* inertial separation chip appears to be very specific for *G. duodenalis* cysts, as 72 % of the cysts were found in the recovered reservoir following the six cycle run. The *Cryptosporidium* inertial separation chip was slightly less specific in comparison to the *Giardia* inertial separation chip; however, it was still quite specific for the *C. parvum* oocyst, as 69 % of them were focused into the recovered reservoir.

The lost (oo)cysts that were not found in either of the reservoirs (waste or recovered) may be attributed to dead volume, which remained within the system and was not pumped out into either of the reservoirs following the run. These lost (oo)cysts represent losses in the concentration efficiency, as their loss directly affects the number of parasites concentrated in the process. This was addressed in early optimisation experiments through the implementation of an additional priming and withdrawal step at the end of the run. However, it appeared that a small percentage of parasites (6-11%) still remained trapped within components of the system, i.e., channels, valves, tubing or syringes.

The small polymer fluorescent beads do not fall in the theoretically range of particles expected to be focused by either of the microfluidic chips that were designed, as they are too small (1.90 µm). They thus acted as non-specific particles which could represent food debris

found in an (oo)cyst suspension following the elution process. The efficiency of the methods in eliminating these undesired particles was high. After cycling the suspensions through the *Giardia* inertial separation chip six times, greater than 70% of the beads were removed, while 56% of the beads were removed following six cycle runs with the *Cryptosporidium* inertial separation chip.

The enumeration of (oo)cysts and beads in the recovered and waste suspensions following one, three and six cycles demonstrated that the loss of parasites to the waste reservoir, observed in previous experiments, occurred due to the gradual loss of un-focused (oo)cysts to the waste reservoir. With each cycle, however, a greater proportion of the undesired particles were eliminated. Thus, depending on the concentration of lettuce/food particles in the suspension, the protocol can be tailored to eliminate either more or less particles, by either increasing or decreasing the number of cycles in the protocol.

5.2 The use of microfluidic inertial separation in the concentration and separation of *G. duodenalis* cysts from lettuce particles

The *Giardia* inertial separation chip and the six cycle concentration and separation protocol was successfully integrated into a conventional method for the detection of *G. duodenalis* cysts on spiked lettuce samples (17). Lettuce was chosen as a food matrix for initial testing, due to its relatively high prevalence of contamination of both *G. duodenalis* cysts and *C. parvum* (17, 64), published detection methodologies, and relatively low number of background food particles, thus theoretically allowing for greater ease of cyst detection. Following optimisation, none of the 18 lettuce samples that were run through the *Giardia* inertial separation chip resulted in any leaking or clogging. In comparison to the conventional method, the

microfluidics method proved to be very effective as both flow cytometry and fluorescence microscopy demonstrated a significant reduction in the number of lettuce particles and other food debris in the final recovered suspensions. Protozoan parasite detection and enumeration by fluorescence microscopy can be a tedious and time-consuming method, especially when analyzing samples with high concentrations of background particles. The sensitivity of detection may also be lower in such samples due to analyst fatigue, and the possible masking of target organisms by debris particles. One of the advantages of the inertial separation method was that it resulted in decreased sample analysis times by fluorescence microscopy. The method was also very efficient and specific for the *G. duodenalis* cysts, as it enabled the recovery of a large proportion (68%) of cysts initially spiked on the lettuce samples and had a limit of detection of 38 cysts per sample. In comparison to the conventional method, the percent recovery was not significantly different and the limit of detection was only slightly higher.

No previous LOD assays using immunofluorescence have been performed for *G. duodenalis* on food, thus the LOD of the method developed by Dixon et al (17) was determined in parallel with the inertial separation method. The slight additional loss of cysts in the new method resulted in a slightly higher LOD when analyzed by immunofluorescence microscopy. However, the additional speed in which the slides were analyzed could allow for the analysis of a greater portion of the sample (> 3 slides), which could lower the 38 cyst LOD obtained from the inertial separation method, and approach that of the conventional method.

In addition to the conventional concentration and separation methods for foods which make use of centrifugation and filters, other in-house methods such as that of Cook et al. (14), incorporate IMS, which also specifically targets *G. duodenalis* and *Cryptosporidium* spp. (oo)cysts. By incorporating IMS following centrifugation, Cook et al. (14) obtained an average

recovery of 46.0 ± 19% for artificially cyst-contaminated leafy green products. A method developed by Robertson and Gjerde (63) involving two washing procedures by rotating drum and sonication, followed by centrifugation and IMS, resulted in an average recovery of 67%. Thus, the average recovery of 68 % of spiked *Giardia* cysts from lettuce samples obtained in the present study, through the use of inertial separation, demonstrates the potential of this technology as an alternative to the more costly and time-consuming IMS-based approaches. Concentration and separation of 10 ml samples using the *Giardia* microfluidic inertial separation chip required 28 min, while the IMS procedure requires 1 hr of antibody incubation alone, not including the additional processing time.

Along with determining the percent recoveries of artificially contaminated salad products, including leafy greens, Cook et al. (14) also examined the relative concentration of background debris on the slides, and designated a rating of high, medium or low. Among 20 different product types, they designated 10 of them as high, 8 as medium and only two as low. This suggests that large numbers of food particles were not eliminated by IMS, making detection by fluorescence microscopy difficult and time-consuming. No direct quantitative comparison studies have been performed on the efficiency of IMS in eliminating unwanted background food particles.

The inertial separation chip, unlike antibodies, does not rely on direct interaction with the cyst and thus is not specific to an epitope-paratope interaction but rather to the size of the cyst. Thus, other species of *Giardia* or *Cryptosporidium* which may not share the same surface markers (epitopes) as *G. duodenalis* cysts or *C. parvum*, but are similar in size, would still be focused by the inertial separation chip and can subsequently be identified.

In addition to improving detection for use with standard immunofluorescence microscopy through the removal of background particles, inertial separation is likely to improve detection by flow cytometry as well. Demonstrating an improved sensitivity with conventional flow cytometry has proven difficult, however, as samples with high numbers of background particles, such as the samples obtained from the conventional methods, contain fluorescent particles of similar size and complexity as the *G. duodenalis* cysts themselves, and thus are difficult to eliminate through gating. Thus, recovered samples with low numbers of cysts approaching the LOD and sampled by conventional methods, often given rise to percent recoveries greater than 100%, indicating the presence of false-positive events (Data not shown). In comparison, samples obtained from the inertial separation method, which contain fewer background food particles, showed lower percent cyst recoveries, which may be attributable to fewer false-positive events. Analyses involving the recent technology of imaging cytometry, which allows for direct visualization of events/particles, may provide more accurate results. It is also anticipated that a microfluidic device such as ours, which can efficiently concentrate and separate particles of interest, will further enhance emerging high-throughput, cost-effective and automated lab on a chip detection platforms, which use molecular-based technologies (53).

5.3 Future directions

Other foods known to be contaminated with *Giardia* cysts, such as berries, have more fragile matrices than lettuce, and when eluted by conventional methods, tend to produce much greater concentrations of food particles, as well as PCR inhibitors. Therefore, studies involving the use of inertial separation on these foods may be expected to yield much cleaner samples, leading to improved detection sensitivity and specificity. Future work, involving other food matrices and PCR detection, would also help determine if the inertial separation microchips are

able to minimize or eliminate PCR inhibitors, thus improving the sensitivity of detection by molecular methods.

The promising results obtain from the integration of inertial microfluidic separation into the detection of *G. duodenalis* cysts have recently led to the design and fabrication of a third version of the *Cryptosporidium* spp. inertial microfluidic chip. As discussed previously, the first and second generations of the microfluidic chips were not yet integrated into a method for the detection of *Cryptosporidium* spp. oocysts on foods, as the increased pressure within the smaller channel would occasionally lead to leaking. This resulted in the implementation of slower working flow rates (0.4 ml/min), which meant six cycle concentrations took 75 min to complete. The next generation of the chip was designed and fabricated specifically to address these issues and to allow for the implementation of the chip into food detection methods. It incorporates 20 parallel inertial separation channels into one microfluidics chip (images in Appendix I). Theoretically, this should result in reduced pressures within the individual channels and, thus, allow for an increased working flow rate of 2.1 ml/min, which ultimately would allow for run times of only 18.5 min. The third generation of the *Cryptosporidium* inertial separation chip is expected to greatly improve the speed and sensitivity of detection of *Cryptosporidium* spp. oocysts on food samples.

Chapter II – Hsp70 gene expression and use as a viability marker for *Cryptosporidium parvum* oocysts under high hydrostatic pressures.

6.0 INTRODUCTION

6.1. High Pressure Processing of *Cryptosporidium* spp.

Currently, there are two published studies which have investigated the effects of high hydrostatic pressure on the viability and infectivity of *Cryptosporidium* spp. As *Cryptosporidium* spp. are protected from the environment by their robust oocyst wall which allows them to survive for extended periods of time in damp and cool conditions such as the surface of foods (62), the need to discover disinfectant processes which reduce their viability/infectivity without altering properties of food such as texture and flavour are needed. A study by Slifko et al. in 2000 (75), investigated the effects of high pressure processing (HPP) on *C. parvum* oocysts in apple and orange juice. They applied a pressure of 550 MPa at hold times ranging from 0-120 sec. To study the effect of the treatment on the viability of the oocysts, they performed an excystation assay as described in the general introduction. To study the effect of the treatment on the infectivity of the oocysts, they performed the foci detection method (FDM) as described in the general introduction. The apple and orange juices had pH values of 3.69 and 3.93, respectively, and the oocysts were in the juices for 48 hr prior to the infectivity assay. Their excystation assay showed that the control samples of oocysts in PBS had a viability of 59%, while that of the oocysts in apple juice was 66%. In the apple juice samples, the viability was reduced to 5% after only 30 sec of HPP treatment at 550 MPa; however, they could not achieve 100% reduction. The study was unable to perform this assay for orange juice, as these samples contained too much pulp and debris to properly identify the empty oocyst shells as well as the sporozoites. The results of the infectivity assay (foci detection method) showed a 3.4 log inactivation following 30 sec of HPP

in apple juice and a >4.1 log inactivation in orange juice following 30 sec of HPP. The article, however, also clarified that food debris in certain apple juice samples may have obstructed possible infection, and the debris inhibited fluorescent antibodies from binding in certain samples that were marked positive for infection. The study also did not distinguish the effects of HPP on viability and infectivity, versus the effects of the juices themselves. Previous articles have demonstrated that storage in juices alone can decrease the viability of *C. parvum* oocysts by as much as 35% in only 24 hr (62). Low pH is one of the major signals for excystation of the oocyst; thus, the low pH of the juices would greatly affect the excystation assay used in the study to examine viability. It would have also been interesting to treat a series of samples of oocysts in PBS solution in order to determine the effect of HPP alone on *C. parvum* viability and infectivity.

A second very interesting study on the effects of HPP on oocysts recovered from experimentally exposed eastern oysters was performed by Collins et al. in 2005 (13), who used the neonatal mouse infectivity assay as a model for infection. A 76-L aquarium containing 12-15 oysters was spiked with 2×10^7 *Cryptosporidium* oocysts. Oysters were collected 24 hr following exposure and were treated at a range of pressures (305 MPa to 550 MPa) and for a different hold times (0-180s). Between 3 and 10 oysters were pooled together and used to feed the mice. Doses thus ranged from 9 to 1,700 oocysts per tested mouse. Thirty mice were infected for each condition and the number of mice infected was used to determine the inactivation of the oocysts by HPP. The results from this study showed that the infectivity of the mice was reduced by at least 40% in every sample which underwent HPP. The samples which underwent 550 MPa for 180 sec showed the greatest reduction in infectivity (93%). The infectivity of the oocysts was shown to decrease with the increase in pressure and hold time.

There have been no published data on the effects of high hydrostatic pressure on *G. duodenalis*, however, a study was performed on the effects of high hydrostatic pressure on *Toxoplasma gondii* oocysts on raspberries (44) and it demonstrated a significant reduction in infectivity following a 60 sec treatment at 340 MPa. Utilising the newly developed hsp70 mRNA viability assay described above, we can better assess the effects of high hydrostatic pressure on the metabolic function of *Cryptosporidium* spp. oocysts, as well as confirm the effects on viability. We can also assess the ability of the assay to quantify viability in contaminated food samples for potential integration into a complete lab on a chip detection system.

6.2 Hypothesis

Cryptosporidium spp. oocysts in buffer and apple cider lose their viability following treatment by high pressure processing.

6.3 Objectives

1. Determine the effect of high hydrostatic pressure on the expression of hsp70 mRNA in *Cryptosporidium* spp. oocysts.

2. Assess the ability of high pressure processing to reduce the viability of *Cryptosporidium* spp. oocysts in PBS using the hsp70 mRNA viability assay.

3. Determine if the hsp70 mRNA viability assay can accurately quantify the percentage of viable oocysts in apple cider.

4. Assess the ability of high pressure processing to reduce the viability of *Cryptosporidium* spp. oocysts in apple cider using the hsp70 mRNA viability assay.

7.0 METHODS

7.1 Parasite isolates

C. parvum oocyst suspensions were purchased from Waterborne, Inc. (New Orleans, LA). The bovine isolate *C. parvum* oocysts were passaged through calves, purified from fecal matter and suspended in phosphate-buffered saline (PBS) with antibiotics. All parasite suspensions were stored at 4°C and used within 4 weeks of shedding.

7.2 Standard curve

The day prior to each trial run, a standard curve for the viability of the *C. parvum* oocysts was created as follows. A portion (240 µl) of the stock suspension of *C. parvum* oocysts (1.25×10^7 per ml) was diluted in 60 µl of 1 X PBS buffer to create a suspension with a concentration of 1×10^7 oocysts per ml. Successive 1 in 10 serial dilutions of this suspension was performed by diluting 30 µl into 270 µl of PBS solution. This was repeated four more times to create suspensions with concentrations ranging from 1×10^7 to 1×10^2 oocysts per ml. Each sample was vortexed for 10 sec and divided into duplicate 100 µl aliquots in individual 1.5 ml Eppendorf test tubes. Duplicate 1×10^7 oocysts per ml control samples were inactivated in a 65°C Thermomixer heating block (Eppendorf, Mississauga, ON) in 10% ammonium. In addition a mixture of 10^5 heat inactivated oocysts and 10^5 viable untreated oocysts were combined into one sample to ensure the assay could accurately determine the correct proportion of viable oocysts in these controls. Each of the 100 µl oocyst samples were subjected to heat shock for 20 min at 45°C in a heating block to induce the expression of the hsp70 gene as recommended by Garces-Sanchez et al. (21).

7.3 mRNA extraction

The extraction of *C. parvum* oocyst mRNA was performed according to the method evaluated and recommended by Garces-Sanchez et al. (21), in which the Dynabeads mRNA DIRECT kit (Invitrogen, Streetsville, ON) is used. Prior to use, 1 mg of Dynabeads were washed with Binding Buffer twice, according to the procedure outlined in the manufacturer's protocol. The extraction was performed according to the manufacturer's protocol, however, following the addition of 1 ml of lithium chloride based lysis/binding buffer to 100 µl of oocysts, a five cycle freeze (liquid N_2, 1 min) – thaw (65°C, 1 min) as recommended by Liang and Keeley (41) was used. Following the freeze-thaw, the residual cell wall components were precipitated by centrifugation (17, 000 x g, 3 min) recommended by Liang and Keeley (41). One ml of the supernatant was mixed with 1 mg of previously washed beads in a sterile 1.5 ml Eppendorf tube and annealing was performed by rotating the tubes on a mixer for 10 min at room temperature. The bead-mRNA complex was then placed on a magnet for 2 min. The suspension was then removed and discarded. The bound bead-mRNA complex was washed twice with Buffer A and B to remove residual contaminants that may have non-specifically bound to the beads. Finally the mRNA was eluted in 15 µl of Tris-HCl buffer by incubating the complex at 75°C for 2 min in a Thermomixer heating block (Eppendorf, Mississauga, ON) to dissociate the mRNA from the beads, then placing the sample on the magnet and immediately transferring the supernatant containing the mRNA to a 0.2 ml RNase-free tube.

7.4 DNase treatment

DNase treatment was performed with the Turbo DNA-free kit (Life technologies, Carlsbad, CA) according to the routine DNase treatment suggested by the manufacturer. This was performed on 15 µl of eluted mRNA through the addition of 1.6 µl of 10 X Turbo DNase buffer and 1 µl of Turbo DNase. The mixture was mixed gently by flicking the tube. The 37°C incubation for 30

min was performed in a BioRad C1000 touch thermal cycler (BioRad, Mississauga, ON). The DNase was inactivated through the addition of 2 µl of DNase inactivation agent provided with the kit, which required a 5-min incubation period at room temperature. The sample was centrifuged at 10, 000 x g to pellet the DNase, and 3 µl of RNA was pipetted from the supernatant.

7.5 cDNA synthesis

Reverse transcription of extracted mRNA was performed with the SuperScript III First-Strand Synthesis System according to the manufacturer's protocol. Initially 3 µl of mRNA, 5 µM of oligo(dT) primer, 1 mM of dNTP mix and DEPC-treated water were added to 0.2 ml PCR tubes (Axygen, Union City, CA) up to a final reaction volume of 10 µl. The mixture was incubated at 65°C for 5 min in a BioRad C1000 touch thermal cycler (BioRad, Mississauga, ON) and then immediately placed on ice for 1 min to allow for the annealing process to occur. The cDNA synthesis mix (10 µl) containing 2 X RT buffer, 10 mM $MgCl_2$, 0.02M DTT, 40 U of RNAseOUT and 200 U of SuperScript III RT was added to the 10 µl of annealed primer/mRNA and placed in the thermocycler for reverse transcription. Cycling conditions consisted of a 50 min synthesis at 50°C followed by a 5 min termination step at 85°C. Following the cDNA synthesis, 1 µl of RNase H was added to the reaction and incubated in the thermocycler for 20 min at 37°C to digest RNA template from the cDNA-RNA hybrid. Duplicate samples containing all the components of the master mix except for the SuperScript III reverse transcriptase, and including RNA template extracted from the 1 x 10^7 oocyst sample, were used as controls to account for any contaminating genomic DNA.

7.6 Real-time PCR

Real-time (quantitative) PCR was performed using a Bio Rad CFX 96 Real-time C1000 thermal cycler (BioRad, Mississauga, ON). The primer/probe set (1PS; forward primer: 5'-AACTTTAGCTCCAGTTGAGAAAGTACTC-3'; reverse primer: 5'-CATGGCTCTTTACCGTTAAAGAATTCC-3'; probe: 5'-FAM-AATACGTGTAGAACCACCAACCAATACAACATC-TAMRA-3') used was designed by Garces-Sanchez et al. (21) and is specific for a 144 bp region of the hsp70 gene. The reaction contained 600 nM of each primer, 300nM of TaqMan probe, 10 µl of 2X SsoAdvance Universal Probes Supermix (BioRad, Mississauga, ON), 2 µl of cDNA and DEPC-treated DNase free water to reach a final reaction volume of 20 µl. Cycling conditions consisted of a 30 sec polymerase activation/denaturation step at 95°C followed by 45 cycles of 15 sec denaturation at 95°C and 1 min of annealing/extension at 60°C. All samples were performed in duplicate. Each of the trials contained no template controls (NTC) and DEPC-treated DNase free water controls. Cycle threshold numbers and baselines were automatically determined by CFX Manager Software version 3.1 (Bio-Rad Laboratories, Inc). Following amplification, the size of the PCR product was determined by running the PCR products on a 2% agarose gel.

7.7 Inoculation of artificially contaminated samples

The fresh-pressed sweet apple cider (President's Choice, Toronto, ON) used in the study was made from a blend of tree-picked Canadian apples, was unfiltered and did not contain any added sugar or preservatives. Using a 10 ml sterile disposable pipette, 9.2 ml of either PBS or apple cider was transferred to a 15 ml Falcon polystyrene conical test tube (BD Biosciences, Franklin Lakes, NJ). The samples were inoculated with 0.8 ml of the original stock *C. parvum* oocysts to create samples with a concentration of 1×10^6 oocysts per ml.

7.8 High pressure processing treatment

Samples were placed in sterilized Whirl-Pak™ bags and heat sealed. The samples were then placed in larger Whirl-Pak™ bags containing approximately 100 ml of 5% bleach and heat sealed once more. Prior to each run, the distilled H_2O in the 1 L pressure chamber of the HPP unit (Dustec high pressure technologies, Wismar, Germany) was heated to 25°C. The unit contains a pressure intensifier pump that reaches a maximum operating pressure of 650 MPa. Following temperature equilibration of the ddH_2O in the pressure intensifier to 25°C, the bag was placed in the pressure chamber and the chamber was sealed with a 250 kg lid. The come up time for the 600 MPa run was 30 sec, followed by hold times of 60, 180 and 300 sec. The come down time was again 30 sec. The 10 ml samples were split following their initial testing 1 hr following HPP treatment and stored at either 4°C or room temperature (21-25°C) in order to examine the effect of storage on *C. parvum* viability and on hsp70 mRNA decay. The maximum temperature reached at one of three positions in the pressure vessel was recorded for each run.

7.9 Hsp70 mRNA production over time

At specific time points (1, 24, 96 and 168 hr) post HPP, 1 ml aliquots of the 10 ml samples were pipetted into 1.5 ml Eppendorf test tubes. The samples were then centrifuged at 2,000 x g for 10 min and 0.9 ml of supernatant was removed. The mRNA extraction process was then performed on the remaining 100 µl of concentrated sample as described above.

7.10 Statistical analysis

Comparative analysis was performed using the student's unpaired t-test to determine if there was a significant difference in oocyst hsp70 mRNA levels produced in response to a 1 min and 5 min high pressure treatment. A student's unpaired t-test was also used to determine if there was a significant difference between the proportion of viable oocysts in the untreated PBS and apple

cider samples. A level of significance of 5% ($\alpha = 0.05$) was used to test for statistical differences. Analysis was done using GraphPad Prism 5, version 5.03 (GraphPad Software, Inc).

8.0 RESULTS

8.1 *C. parvum* hsp70 mRNA expression in response to high hydrostatic pressures

Hsp70 mRNA has been shown to be expressed by viable *Cryptosporidium* spp. oocysts that are subjected to certain levels of heat, thus signalling its potential use as a viability marker. It has also been shown, however, that other stressors such as various oxidants can also induce its transcription. The hsp70 mRNA viability assay will likely lead to an over-estimation of oocyst viability, if used immediately following exposure to a stress which induces its expression, such as an inactivation treatment. This is because immediately following treatment, the hsp70 mRNA expressed in response to the stress are still likely to be present in the oocysts, as there has not been sufficient time to allow for their degradation within the cell. Thus, elevated levels of hsp70 mRNA are likely to be detected in oocysts that are no longer viable following a stress treatment. This may prevent its immediate use as a viability marker in response to certain inactivation treatments. In fact, this was shown to be the case for *C. parvum* oocysts treated with various chlorine-based oxidants (5). However, using a time course assay, the authors determined that the hsp70 mRNA transcribed during the treatment would begin to decay and, by approximately 24 hr, would return close to basal levels of expression. Thus, prior to using the hsp70 mRNA viability assay to determine the viability of oocysts following HPP, it is important to examine the effect of high hydrostatic pressures on hsp70 mRNA expression.

Prior to any high pressure processing of samples, a standard curve of the stock suspension of *C. parvum* oocysts used to spike the samples was performed within a maximum of 24 hr prior to treatment. Figure 19 is a representative standard curve generated from the qRT-PCR of the *C. parvum* hsp70 mRNA prior to the initial HPP treatment. The sensitivity of the method was determined to be 100 oocysts per sample (1,000 oocysts/ml). In addition to using

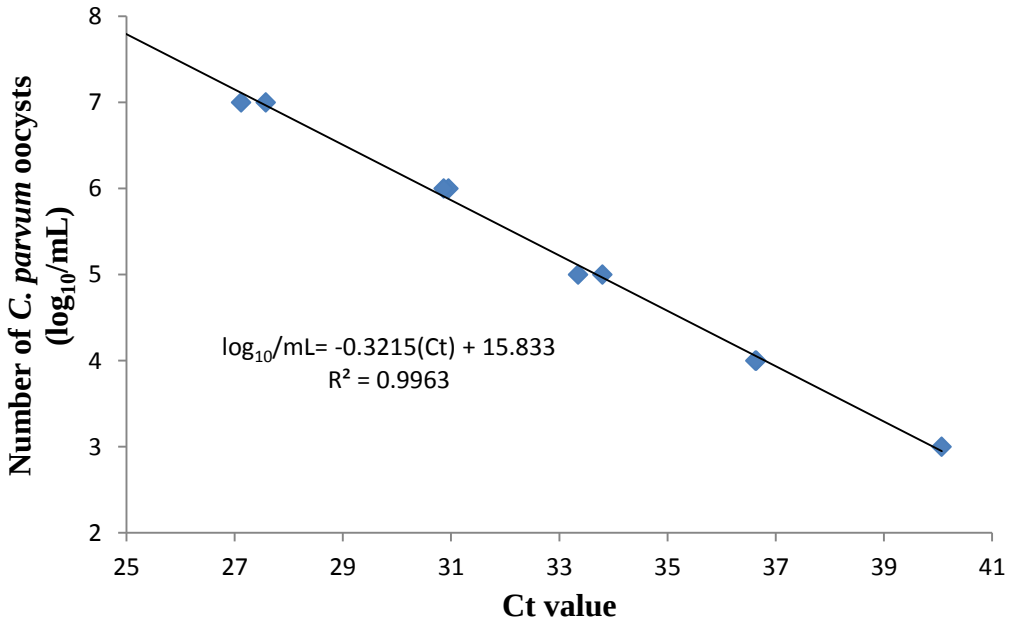
Number of C. parvum oocysts (log10/mL)
8
7
6
5
4
3
2
log10/mL= -0.3215(Ct) + 15.833
R² = 0.9963
25
27
29
31
33
35
37
39
41
Ct value

Fig. 19 Standard curve for *C. parvum* oocysts as determined by qRT-PCR targeting hsp70 mRNA. Standard curve generated for trial 1. Duplicate samples of *C. parvum* oocysts in PBS were prepared at each inoculum level. Each sample was quantified in duplicate and the data points represent the average Ct value.

duplicate samples with concentrations ranging from 10^2-10^7 oocysts per ml, suspensions of 10^7 oocysts per ml were inactivated as controls and had Ct values greater than 45. To ensure that the PCR was specific to the 144 bp fragment of the *Cryptosporidium* spp. hsp70 gene, and that no additional non-specific amplification was occurring, the products of the qRT-PCR were run on a gel and PCR bands of the expected lengths were identified (Fig. 20). A band was absent in lane 9 for one of the duplicate samples containing 1,000 oocysts, however, this was expected as the sample had a Ct value greater than 45 and this concentration of oocysts is approaching the limit of detection for the qRT-PCR assay. The maximum temperature reached in the pressure vessel was recorded for each run and reached a maximum of 36.2°C during the runs with 5 min hold times. Exposure to this temperature for a few minutes should not have any significant effect on the viability of the oocysts.

The relative hsp70 mRNA levels produced in response to HPP significantly increased ($p<0.05$) as the hold time increased from 1 to 5 min (Fig. 21). Thus it seems that high hydrostatic pressure induces the transcription of hsp70 mRNA. When correlated with the number of viable oocysts in each sample it indicates that more viable oocysts are present in the samples that underwent the harsher HPP treatment, which is counter intuitive to what one would think and is also not supported by the current literature. Therefore, in order to obtain an accurate assessment of the ability of the hsp70 mRNA viability assay to determine the inactivation of *C. parvum* oocysts, another time point must be used which allows sufficient time for decay of the mRNA produced to occur.

8.2 Time course of viable oocysts in PBS stored at 4°C or room temperature

Ten ml aliquots of PBS containing 10^6 oocysts per ml were either untreated or treated with HPP. The hsp70 mRNA viability assay was performed immediately following treatment on 1 ml

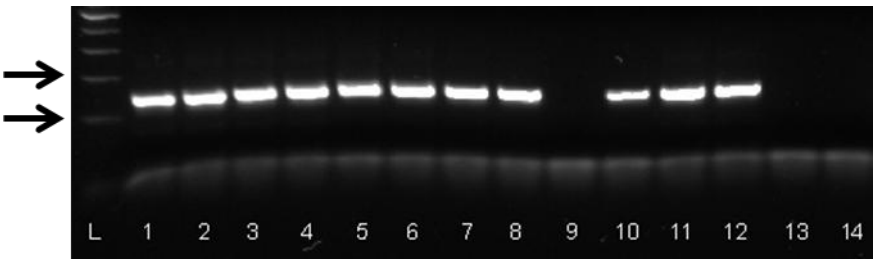
L 1 2 3 4 5 6 7 8 9 10 11 12 13 14

Fig. 20 qRT-PCR amplification products generated from the standard curve are specific to the *Cryptosporidium* spp. hsp70 gene. Products generated from the qRT-PCR of a 144 bp region of the hsp70 gene were run on a 2% polyacrylamide gel (40 min at 100V). Lanes 1-10 represent 10^7-10^3 *C. parvum* oocysts samples in duplicate, lanes 11-12 represent 10^5 oocysts mixed with 10^5 heat inactivated oocysts, lanes 13-14 represent 10^5 heat inactivated oocysts and lane L represents a 100-bp DNA ladder. Upper and lower arrows correspond to band sizes of 200 and 100 bp, respectively.

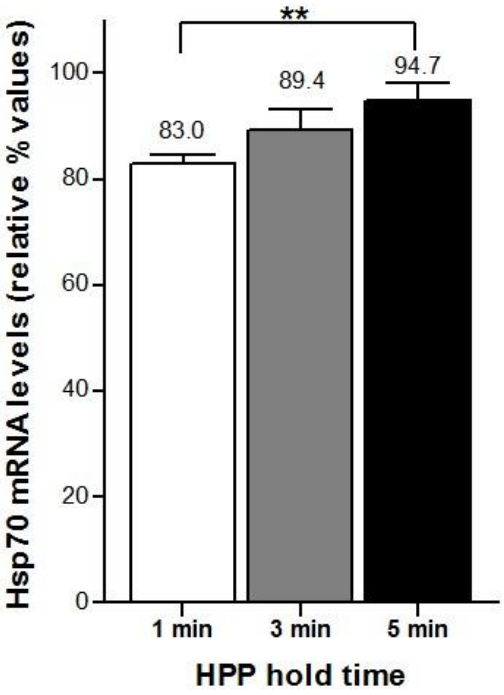
**
94.7
89.4
83.0
100
80
60
40
20
0
Hsp70 mRNA levels (relative % values)
1 min
3 min
5 min
HPP hold time

Fig. 21 High hydrostatic pressures induce hsp70 mRNA transcription in *C. parvum* oocysts. 100% hsp70 mRNA level corresponds to the level of heat-induced hsp70 mRNA amplification from a 10^6 untreated oocyst sample. Samples of 10^6 oocysts were prepared in PBS and were subjected to high pressure processing at 600 MPa for hold times of 1, 3 and 5 min. Error bars represent the SD from three independent experiments.**$p \leq 0.01$.

aliquots of each sample. Of the remaining 9 ml of each sample, half was stored at 4°C while the remaining half was stored at room temperature. As eukaryotic mRNA degradation machinery (i.e., deadenylases, decapping nucleases, endoribonucleases and exoribonucleases) exhibit optimal activity at physiological temperatures (37°C), storage at temperatures less than this are likely to result in slower degradation rates. Thus the storage temperature following treatment is likely to influence which time point the hsp70 mRNA levels return to their basal level, with the expectation that the samples stored at room temperature will return to their basal levels sooner. The viability of the samples were thus assessed 1, 24, 96 and 168 hr post treatment in order to provide a time course of the hsp70 mRNA expression in the oocysts.

As seen in the previous experiment, immediately following treatment, the hsp70 mRNA viability assay demonstrated that the HPP-treated sample with a hold time of 5 min contained the highest number of viable oocysts (highest mRNA expression level) in the treated samples (5.52 $\log_{10}$ viable oocysts per ml), while the untreated sample demonstrate an expected 6.02 $\log_{10}$ viable oocysts per ml (Fig. 22). The samples treated at hold times of 1 and 3 min contained 5.05 and 4.81 $\log_{10}$ viable oocysts per ml, respectively. However, 24 hr post treatment, in both sample sets stored at 4°C and room temperature, the viability of most of the treated samples decreased in comparison to the untreated control samples. This seems to indicate that the initial hsp70 mRNA levels detected were most likely in response to the high hydrostatic pressures and not the heat induction. The elevated hsp70 mRNA levels were likely interfering with the viability assay and over-estimated the number of viable oocysts initially. However 24 hr following HPP treatment, the hsp70 mRNA levels expressed in response to the high hydrostatic pressures must have begun to degrade. Then, at 96 hr post-treatment, the viability of the oocysts in the HPP-treated samples decreased slightly in the samples stored at 4°C and decreased greatly in the samples stored at

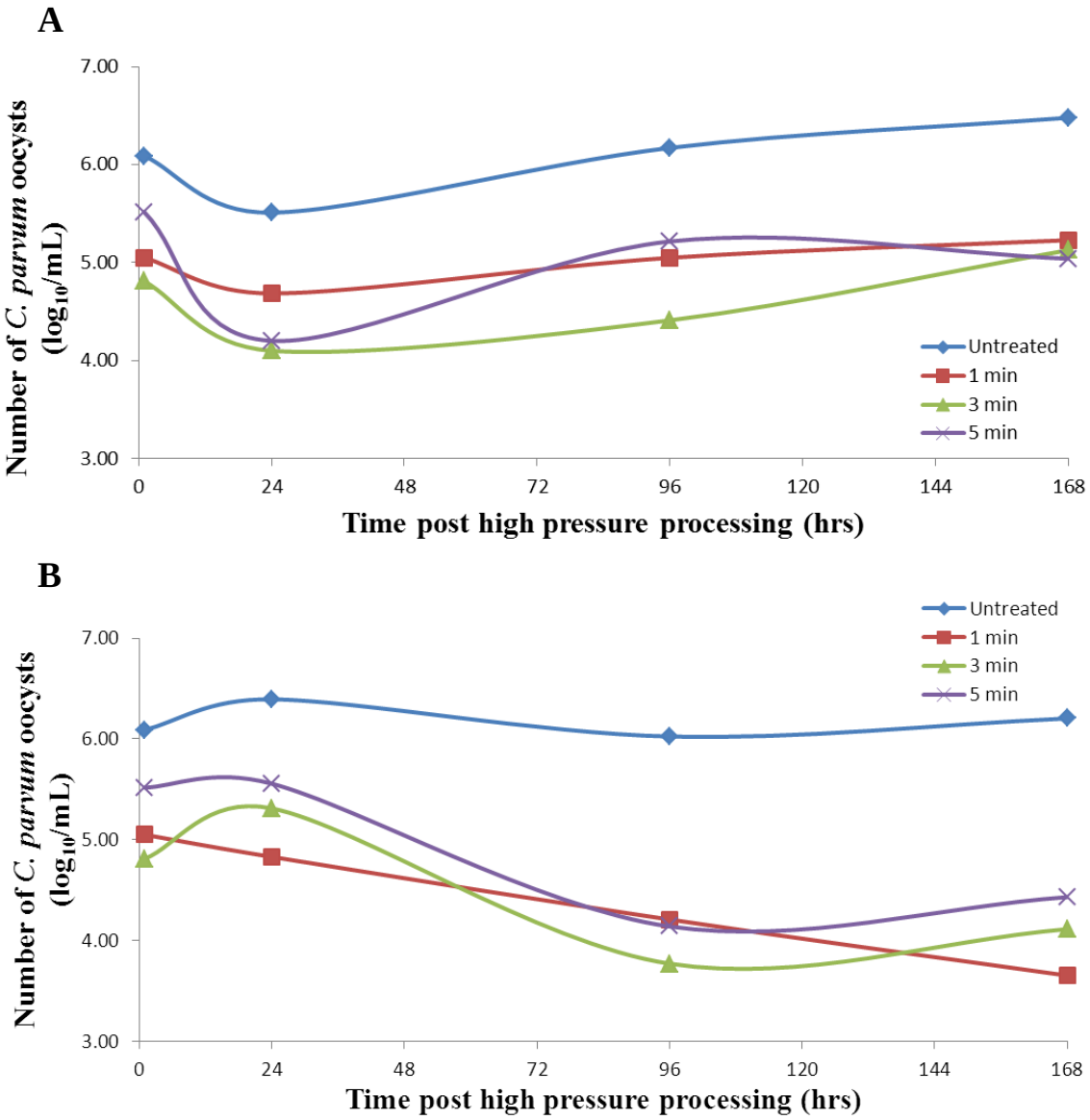
A
7.00
6.00
5.00
4.00
3.00
Number of C. parvum oocysts (log10/mL)
0
24
48
72
96
120
144
168
Time post high pressure processing (hrs)
Untreated
1 min
3 min
5 min
B
7.00
6.00
5.00
4.00
3.00
Number of C. parvum oocysts (log10/mL)
0
24
48
72
96
120
144
168
Time post high pressure processing (hrs)
Untreated
1 min
3 min
5 min

Fig. 22 Time course of the number of viable *C. parvum* oocysts following high pressure processing. Samples containing 10^6 oocysts in PBS were either untreated or treated with high pressure processing at 600 MPa for 1, 3 and 5 min. Samples were subjected to heat shock, lysed and processed for hsp70 qRT-PCR. Samples were processed immediately following treatment or were stored at 4°C (A) or room temperature (B), and processed at 24, 96 and 168 hr post treatment.

room temperature. At 96 hr post-treatment, it finally appeared that the viability of the oocysts in comparison to those in the untreated samples stabilized, as there was not much difference in viability in comparison to the control at the 168 hr time point. Thus, it appears that performing the hsp70 mRNA viability assay 4 days post-treatment, provides the most accurate representation of the number of viable oocysts in a sample as the hsp70 mRNA produced in response to the high hydrostatic pressure stress has had sufficient time to decay. The results also indicate that the samples stored at room temperature allowed for a higher rate of decay of hsp70 mRNA as the difference in viability was greatest in these samples and the untreated control sample did not exhibit any reductions in viability from storage at room temperature over the one week period (Fig. 22B).

8.3 Inactivation of *C. parvum* oocysts in PBS and apple cider following HPP

Apple cider samples containing 10^6 oocysts per ml were treated with HPP for 1, 3 and 5 min at 600 MPa, stored at room temperature and analyzed with the viability assay four days post-treatment. The artificially-contaminated apple cider samples had $\log_{10}$ oocyst inactivations of 2.29 following the 1 min of hold time, 2.53 following 3 min, and 2.81 following 5 min (Fig. 23). This corresponds to reductions in viability of 99.80-99.94%. The $\log_{10}$ oocyst inactivation appears to increase slightly as the hold time increased. The PBS samples analyzed 4 days post treatment had $\log_{10}$ oocyst inactivations of 1.86 ± 0.06 (n=2) following the 1 min of hold time, 2.29 ± 0.05 (n=2) following 3 min and 1.73 ± 0.21 (n=2) following 5 min (Fig. 23). Thus, with the PBS samples, an increase in hold time does not necessarily result in an increase in the inactivation of oocysts. In addition, the inactivation of oocysts was slightly greater in the apple cider samples than in the PBS samples. This increase in inactivation is not a result of storage of

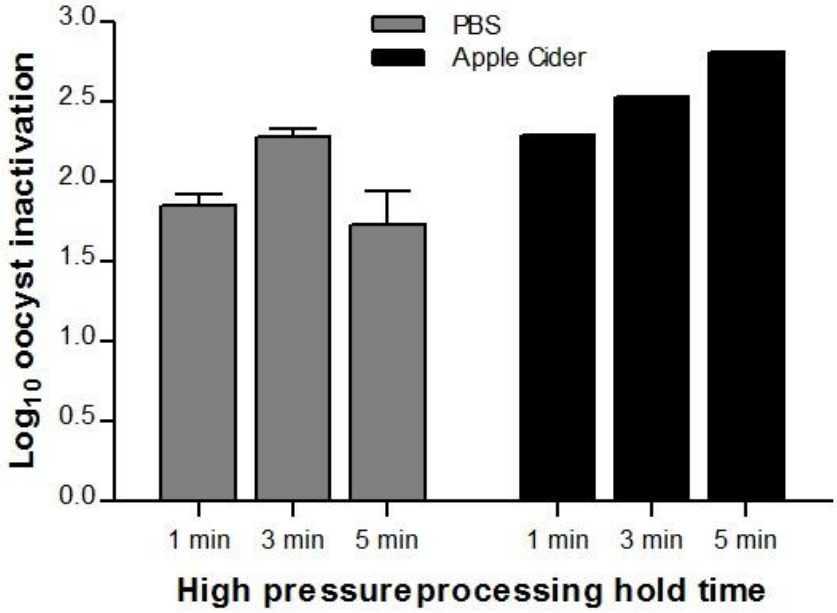
PBS
Apple Cider
3.0
2.5
2.0
1.5
1.0
0.5
0.0
Log10 oocyst inactivation
1 min
3 min
5 min
1 min
3 min
5 min
High pressure processing hold time

Fig. 23 Inactivation of *C. parvum* oocysts in PBS and apple cider treated with 600 MPa of pressure. Samples of 10^6 oocysts were held at 600 MPa for hold times of 1, 3 and 5 min, kept at room temperature and evaluated 4-days post-treatment. The results are interpreted in $\log_{10}$ inactivation values using the formula $\log_{10}$ inactivation = $\log_{10}(N_u) - \log_{10}(N_t)$, where N_u is the number of viable oocysts found in the untreated sample and N_t is the number of viable oocysts in the sample that underwent high pressure processing. Apple cider samples treated for 1 min were evaluated 2-days post-treatment instead of 4.

the oocysts in the apple cider, a suspension with low a pH, as the $\log_{10}$ inactivations were calculated in relation to the untreated oocyst sample which was also stored in apple cider at room temperature.

9.0 DISCUSSION

9.1 Use of the hsp70 mRNA viability assay for HPP treated oocysts in apple cider

The *C. parvum* hsp70 mRNA expression seen in response to high hydrostatic pressure stress supports what was found in the study by Bajszar and Dekonenko (5), in which they examined the response to chlorine-based oxidants. They found that as the length of time in which the oocysts were exposed to the oxidant increased, the amount of hsp70 mRNA produced by the *C. parvum* oocyst in response increased. This was also seen in the present study, in which the increase in exposure time to high hydrostatic pressure (hold time), lead to an increase in hsp70 mRNA transcription. Thus, high hydrostatic pressure induces the expression of hsp70 mRNA. This prevents the accurate determination of oocyst viability through the use of the hsp70 mRNA assay immediately following HPP treatment. Bajszar and Dekonenko (5), however, found that following storage at room temperature the hsp70 mRNA induced by a heat or oxidant stress decayed within 12-16 hr and returned to its basal level by 24 hr. Although this was seen to a certain extent in the time course assay performed in the present study, the majority of the decay occurred starting 24 hr following treatment and did not stabilize until 4-days post-treatment. Therefore it seems that a determination of the viability of the oocysts in a sample can be determined 4 days post treatment with the hsp70 mRNA viability assay.

The assay was also successful in determining the viability of oocysts in apple cider samples, as 10^6 oocyst suspensions taken from the same stock suspension were added to 10 ml of PBS and 10 ml of apple cider, and there was no significant difference ($p>0.05$) in average oocyst viability between the samples over three time points. The untreated apple cider sample containing 10^6 oocysts per ml had an average of 6.21 ± 0.18 $\log_{10}$ ($n=3$) viable oocysts, while the

untreated PBS sample with the same concentration of oocysts had an average of 6.07 ± 0.23 $\log_{10}$ (n=3) viable oocysts.

9.2 Use of HPP as an inactivation treatment for *Cryptosporidium* spp. oocysts

As previously mentioned, there has currently been only one study which has examined the effects of HPP on *Cryptosporidium* spp. oocyst viability in apple cider (75). The results of this study seem to support the reduction in viability observed by Slifko et al. (75), which used the excystation assay and HPP at 550 MPa. That study similarly observed that increasing the hold time of HPP slightly increased the reduction in viability. They found that the oocysts had a 5% viability following HPP with a hold time of 30 sec, and that the viability decreased by a few percent upon increasing the hold time. The initial suspension of oocysts, however, only had 66% viability. Thus, they only observed a reduction in viability of 61% following 30 sec of treatment, and approximately 64% following their longest treatment of 120 sec. The current study, in comparison, obtained a 99.80% reduction following a 1 min treatment, and approached 99.94% reduction following the longest (5 min) treatment. Although the pressure was increased slightly from 550 MPa used in the Slifko et al. (75) study to 600 MPa , which may account for the differences seen between the two viability assays, it is likely that the increased reduction in viability which was obtained with the hsp70 mRNA viability assay is due to the increased accuracy of the assay. This is likely because, as discussed in greater detail below, the results obtained from the hsp70 viability assay seem to correlate better with the results of infectivity assays, in comparison to other viability assays.

Slifko et al. (75) also performed HPP on spiked orange juice samples. However, the excystation method did not allow for the determination of the reduction in viability of the samples, as they contained too much pulp and debris which interfered with the

immunofluorescence microscopy used in the excystation viability assay. However, it is possible that the hsp70 mRNA viability assay, utilising qRT-PCR, would not encounter these same problems and, assuming no PCR inhibition, it could accurately determine the effects of HPP on contaminated orange juice samples.

The study by Slifko et al. (75) also determined the number of infectious *C. parvum* oocysts remaining after HPP treatment, through the use of the FDM cell culture infectivity assay. Following 30 sec of HPP treatment, they observed a 3.4 $\log_{10}$ inactivation and complete inactivation following 60 sec of HPP (>4.2 $\log_{10}$ inactivation). These $\log_{10}$ inactivations are greater than what was observed in the current study, as 1 and 5 min of HPP treatment only resulted in inactivations of 2.29 $\log_{10}$ and 2.81 $\log_{10}$ respectively. However, it does seem that the results of the hsp70 mRNA viability assay more closely correlate with the results of infectivity assays than those of excystation assays. It has also been previously observed that oocyst infectivity decreased slightly more rapidly than their viability (55) which would account for the higher inactivations seen in the FDM infectivity assay in comparison to the hsp70 viability assay.

The second study performed on the effects of HPP on *C. parvum* oocyst infectivity (13) used the mouse pup animal model and found decreases in infectivity of 83% following 1 min of HPP at 550 MPa and 93.3% following 3 min. The results of the viability assay performed in the present study support these reductions in infectivity. Interestingly, as the hold time was increased to 4 and 6 min, the reduction in viability decreased to 65% and 80%, respectively, which corresponded to more viable oocysts in those samples than the samples with shorter hold times. This was not observed with the apple cider samples, as the 5 min treatment resulted in the highest reduction in viability; however, this was seen in the PBS samples, as the 3 min treatment

resulted in the highest reduction. As the animal infectivity study involved oysters, perhaps the matrix plays a role in determining the optimal hold time for HPP.

Slifko et al. (75) obtained a >4.1 $\log_{10}$ reduction in infectious oocysts in both apple and orange juice, thus leading them to conclude that HPP rendered the oocysts non-viable and non-infectious, suggesting that HPP is a suitable alternative to thermally-treating juice. Collins et al. (13) concluded that of the 900 to 1,700 oocysts treated with HPP and fed to the mouse pups, a maximum inactivation of 93.3% was achieved. Thus, they concluded that HPP shows promise as an alternative to other treatment (inactivation) methods in the control of *Cryptosporidium* spp. on foods. The results from the present study seem to support the results and conclusion of Collins et al. (13). Although reductions in viability of 99.94% were achieved after treatment, this only translated in a 2.81 $\log_{10}$ reduction in oocysts. Thus, any food sample contaminated with 5 $\log_{10}$ viable oocysts or greater would still contain sufficient viable, and most likely infectious oocysts to cause infection in humans (ID_{50} of 132 oocysts). This study shows the potential of HPP as a non-thermal alternative for the control of *Cryptosporidium* spp. oocysts on certain foods that are contaminated with less than 4 $\log_{10}$ of viable oocysts, which is the case for the majority of foods contaminated with *Cryptosporidium* spp. It does not, however, meet the current 5 $\log_{10}$ reduction required by the FDA for most other pathogens found in juices.

9.3 Future Directions

As the hsp70 mRNA viability assay seems to support results from the infectivity assays and has proven to be an accurate, sensitive, cost-effective, high-throughput and rapid tool to quantify the viability of *Cryptosporidium* spp. oocysts, studies on its potential as a viability assay for other protozoan parasites such as *G. duodenalis* would also be of great interest. In addition, as most elution, concentration and detection methods are designed to detect both

Cryptosporidium spp. oocysts and *G. duodenalis* cysts, creating a viability assay targeting both protozoan parasites would be of value. A viability assay for *G. duodenalis* cysts as well as *C. parvum* oocysts targeting the hsp70 mRNA in a multiplex RT-PCR assay has been developed (52); however, designing a primer and probe set specific for use with quantitative RT-PCR would be more significant.

Further use of the hsp70 mRNA viability assay to determine the potential of HPP in reducing the viability of oocysts found in foods, such as orange juice, which have proven to be difficult to analyse by current viability or infectivity assays, would also be of interest.

Liang and Keeley (41) directly compared the effectiveness of the hsp70 mRNA viability assay to a viability assay making use of propidium monoazide (PMA), a photoactive vital dye, which can only penetrate into membrane-compromised or dead cells, and concluded that targeting the hsp70 mRNA was more efficient in environmental samples. Studies such as Bajszar and Dekonenko (5), which have directly compared the results of the hsp70 mRNA viability assay to the results of the FDM tissue culture infectivity assay, have found very high correlations. To further support the use of the hsp70 mRNA assay as an indicator of oocyst infectivity, a study is needed which directly compares the method to an animal infectivity assay.

10.0 GENERAL CONCLUSIONS

Cryptosporidiosis and giardiasis cause significant health problems to humans in North America and worldwide. Detecting *Cryptosporidium* spp. oocysts and *Giardia duodenalis* cysts in both water and on foods, determining their molecular characteristics, and viability are essential in determining prevalence levels in those matrices, possible sources of contamination and, ultimately, routes of transmission to humans. Data of this type will help to inform health risk assessments and the development of strategies and policies aimed at preventing the spread of these diseases and reducing their prevalence in the population. The work performed in this study

directly furthers both the fields of food microbiology and protozoan parasitology, as it demonstrates the potential of lab on a chip technology in improving detection and viability determination methods for *Cryptosporidium* spp. and *Giardia duodenalis*. This technology and these methods can also be applied to water and environmental samples as well as to other protozoan parasites such as *Toxoplasma gondii* or *Cyclospora cayetanensis*.

There are currently no standardized and validated methods for the detection of *Cryptosporidium* spp. or *Giardia duodenalis* on foods. Conventional methods for the concentration of protozoan parasites from foods are based on the (oo)cysts specific gravities and thus use centrifugation, which is non-specific and concentrates a number of un-wanted particles as well. This study has shown that these conventional methods can produce high recovery rates and low limits of detection when analyzed by microscopy; however, they also give rise to samples with high concentrations of food particles, which increase analysis times and often affect the accuracy and sensitivity of downstream detection, viability and infectivity methods. Results of this work show the effectiveness of microfluidic inertial separation in the removal of lettuce particles which interfered with parasite detection by immunofluorescence microscopy and flow cytometry. This method is also likely to remove potential PCR inhibitors that often arise from the processing of foods, which is expected to improve the sensitivity of molecular-based detection techniques such as PCR.

Current viability assays making use of DAPI or PI vital dyes, or *in vitro* excystation, often overestimate the viability of *Cryptosporidium* spp. oocysts in comparison to the gold standard animal infectivity assays. The present study supports the use of the hsp70 mRNA viability assay as a more accurate determination of viability, as it correlates more closely with results obtained by animal infectivity assays. This study also demonstrates, for the first time, the

utility of the assay in determining the viability of oocysts on food. Although the potential exists for the use of HPP in the treatment of apple cider samples contaminated with *Cryptosporidium* spp., it appears that the robust oocyst life form of the parasite is much more resistant to high hydrostatic pressures than other pathogens, as the log reduction resulting from treatment was not as high.

Much of the work that has been performed has been aimed at developing a complete lab on a chip system. It is anticipated that this technology will allow for the rapid, automated, low cost and high-throughput testing of foods possibly contaminated with protozoan parasites. This type of detection system would allow for more robust surveillance and prevalence studies as a greater number of food samples could be analyzed in a shorter time period, at a lesser financial cost, and with reduced hands-on technician time. The ability to efficiently concentrate protozoan parasite suspensions through the use of microfluidic devices, as demonstrated in this study, greatly furthers the development of a lab on a chip system. In addition, due to the existence of real-time PCR assays that have previously been integrated into microfluidic platforms, the potential also exists to integrate the hsp70 mRNA detection assay for viable protozoan parasites. A lab on a chip system consisting of the concentration, separation and detection components would allow for the detection of viable (oo)cyst in suspensions heavily contaminated with background debris, such as food samples, which have previously been shown to be difficult with most other viability/infectivity assays. Further work is still needed, however, to obtain a complete lab on a chip system.

Future work may involve the implementation of a miniaturized flow cytometer to detect and enumerate cysts and oocysts. The concentrated parasite suspension arising from the inertial separation chip would next need to be pumped into a microchip containing the fluorescent

antibodies developed against *Cryptosporidium* spp. oocysts and *Giardia duodenalis* cysts. The microchip could also be placed on one of the many miniaturized heating blocks currently available for lab on a chip systems, thus allowing for optimised antibody-antigen binding at 37ºC. Once *Cryptosporidium* spp. oocysts and *Giardia duodenalis* cysts are bound to fluorescent antibodies, the suspension would be pumped through a miniaturized microfluidic flow cytometer, which has currently also been developed, and cysts and oocysts could be detected. This detection system would be very rapid in comparison to standard PCR detection methods. Following detection of protozoan parasites, further characterisation can be performed. The protozoan parasites could be heat-shocked and pumped into a PCR microchip containing all the necessary reagents to perform a multiplex hsp70 qRT-PCR. This would allow for the enumeration of the viable *Cryptosporidium* spp. oocysts and *Giardia duodenalis* cysts in the food suspension using the hsp70 mRNA viability assay. Once more these chips would be placed on the miniaturized heating block already contained in the system. Genotyping of the detected protozoan parasites could additionally be performed using a PCR microchip to amplify target regions of the genome and detecting the specific products in a microarray chip. The microarray could be designed to target multiple species and genotypes of *Cryptosporidium* and *Giardia* protozoan parasites. Much of the technology needed to perform this future work is currently available, and is in use in lab on a chip detection systems for certain microbial pathogens. For example, Yang et al. (87) have developed a complete lab on a chip system capable of viral sample purification and detection making use of the mini flow cytometer. The challenge will be integrating these individual chips into a complete lab on a chip system designed to deal with the difficulties presented by various food matrixes and the complex protozoan parasites themselves.

REFERENCES

1. Akiyoshi, D., X. Feng, M. Buckholt, G. Widmer, and S. Tzipori. 2002. Genetic analysis of a *Cryptosporidium parvum* human genotype 1 isolate passaged through different host species. Infect. Immun. **70:**5670-5675. doi: 10.1128/IAI.70.10.5670-5675.2002.

2. **Ankarklev, J., J. Jerlstrom-Hultqvist, E. Ringqvist, K. Troell, and S. G. Svard.** 2010. Behind the smile: cell biology and disease mechanisms of *Giardia* species. Nature Reviews Microbiology. **8:**413-422. doi: 10.1038/nrmicro2317.

3. **Avila, K., D. Moxey, A. de Lozar, M. Avila, D. Barkley, and B. Hof.** 2011. The onset of turbulence in pipe flow. Science. **333:**192-196. doi: 10.1126/science.1203223.

4. **Baishanbo, A., G. Gargala, A. Delaunay, A. Francois, J. Ballet, and L. Favennec.** 2005. Infectivity of *Cryptosporidium hominis* and *Cryptosporidium parvum* genotype 2 isolates in immunosuppressed Mongolian gerbils. Infect. Immun. **73:**5252-5255. doi: 10.1128/IAI.73.8.5252-5255.2005.

5. **Bajszar, G., and A. Dekonenko.** 2010. Stress-induced hsp70 gene expression and inactivation of *Cryptosporidium parvum* oocysts by chlorine-based oxidants. Appl. Environ. Microbiol. **76:**1732-1739. doi: 10.1128/AEM.02353-09.

6. **Beckmann, R., L. Mizzen, and W. Welch.** 1990. Interaction of hsp70 with newly synthesized proteins - Implications for protein folding and assembly. Science. **248:**850-854. doi: 10.1126/science.2188360.

7. **Benere, E., T. Geurden, L. Robertson, T. Van Assche, P. Cos, and L. Maes.** 2010. Infectivity of *Giardia duodenalis* Assemblages A and E for the gerbil and axenisation of duodenal trophozoites. Parasitol. Int. **59:**634-637. doi: 10.1016/j.parint.2010.08.001.

8. **Bingham, A., E. Jarroll, and E. Meyer.** 1979. *Giardia* sp - Physical factors of excystation *in vitro*, and excystation vs eosin exclusion as determinants of viability. Exp. Parasitol. **47:**284-291. doi: 10.1016/0014-4894(79)90080-8.

9. **Bingham, A., and E. Meyer.** 1979. *Giardia* excystation can be induced *in vitro* in acidic solutions. Nature. **277:**301-302. doi: 10.1038/277301a0.

10. **Budu-Amoako, E., S. J. Greenwood, B. R. Dixon, H. W. Barkema, and J. McClure.** 2011. Foodborne illness associated with *Cryptosporidium* and *Giardia* from livestock. Journal of Food Protection®. **74:**1944-1955.

11. **Buret, A. G., and J. Cotton.** 2011. Pathophysiological processes and clinical manifestation of giardiasis, p. 301. *In* H. D. Lujan and S. Staffan (eds.), *Giardia* A model Organism. SpringerWienNewYork, New york.

12. **Carranza, P. G., and H. D. Lujan.** 2010. New insights regarding the biology of *Giardia lamblia*. Microb. Infect. **12:**71-80. doi: 10.1016/j.micinf.2009.09.008.

13. **Collins, M., G. Flick, S. Smith, R. Fayer, R. Croonenberghs, S. O'Keefe, and D. Lindsay.** 2005. The effect of high-pressure processing on infectivity of *Cryptosporidium parvum* oocysts recovered from experimentally exposed Eastern oysters (Crassostrea virginica). J. Eukaryot. Microbiol. **52:**500-504. doi: 10.1111/j.550-7408.2005.00059.x.

14. **Cook, N., R. A. B. Nichols, N. Wilkinson, C. A. Paton, K. Barker, and H. V. Smith.** 2007. Development of a method for detection of *Giardia duodenalis* cysts on lettuce and for simultaneous analysis of salad products for the presence of *Giardia* cysts and *Cryptosporidium* oocysts. Appl. Environ. Microbiol. **73:**7388-7391. doi: 10.1128/AEM.00552-07.

15. **Di Carlo, D., D. Irimia, R. G. Tompkins, and M. Toner.** 2007. Continuous inertial focusing, ordering, and separation of particles in microchannels. Proc. Natl. Acad. Sci. U. S. A. **104:**18892-18897. doi: 10.1073/pnas.0704958104.

16. **Dixon, B. R.** 2014. Transmission dynamics of foodborne parasites in produce. *In* A. Gajadhar (ed.), Foodborne Parasites in the Food Supply Web: Occurrence and Control, vol. 15. Woodhead Publishing Ltd, Cambridge, UK.

17. **Dixon, B., L. Parrington, A. Cook, F. Pollari, and J. Farber.** 2013. Detection of *Cyclospora*, *Cryptosporidium*, and *Giardia* in ready-to-eat packaged leafy greens in Ontario, Canada. J. Food Prot. **76:**307-313. doi: 10.4315/0362-028X.JFP-12-282.

18. **Dupont, H., C. Chappell, C. Sterling, P. Okhuysen, J. Rose, and W. Jakubowski.** 1995. The Infectivity of *Cryptosporidium parvum* in healthy-volunteers. N. Engl. J. Med. **332:**855-859. doi: 10.1056/NEJM199503303321304.

19. **Fayer, R., and L. Xiao.** 2008. *Cryptosporidium* and Cryptosporidiosis. IWA publishing, Boca Raton, FL.

20. **Feng, Y., and L. Xiao.** 2011. Zoonotic potential and molecular epidemiology of *Giardia* species and giardiasis. Clin. Microbiol. Rev. **24:**110-140. doi: 10.1128/CMR.00033-10; 10.1128/CMR.00033-10.

21. **Garces-Sanchez, G., P. A. Wilderer, J. C. Munch, H. Horn, and M. Lebuhn.** 2009. Evaluation of two methods for quantification of hsp70 mRNA from the waterborne pathogen *Cryptosporidium parvum* by reverse transcription real-time PCR in environmental samples. Water Res. **43:**2669-2678. doi: 10.1016/j.watres.2009.03.019.

22. **Giles, M., K. Webster, J. Marshall, J. Catchpole, and T. Goddard.** 2001. Experimental infection of a lamb with *Cryptosporidium parvum* genotype 1. Vet. Rec. **149:**523-525.

23. **Gillin, F., and L. Diamond.** 1980. Clonal growth of *Giardia lamblia* trophozoites in semisolid agarose medium. J. Parasitol. **66:**350-352. doi: 10.2307/3280836.

24. **Gillin, F., D. Reiner, M. Gault, H. Douglas, S. Das, A. Wunderlich, and J. Sauch.** 1987. Encystation and expression of cyst antigens by *Giardia lamblia in vitro*. Science. **235:**1040-1043. doi: 10.1126/science.3547646.

25. **Girouard, D., J. Gallant, D. Akiyoshi, J. Nunnari, and S. Tzipori.** 2006. Failure to propagate *Cryptosporidium* spp. in cell-free culture. J. Parasitol. **92:**399-400. doi: 10.1645/GE-661R.1.

26. **Harris, J., and F. Petry.** 1999. *Cryptosporidium parvum*: Structural components of the oocyst wall. J. Parasitol. **85:**839-849. doi: 10.2307/3285819.

27. **Hijjawi, N., A. Estcourt, R. Yang, P. Monis, and U. Ryan.** 2010. Complete development and multiplication of *Cryptosporidium hominis* in cell-free culture. Vet. Parasitol. **169:**29-36. doi: 10.1016/j.vetpar.2009.12.021.

28. **Hijjawi, N., B. Meloni, M. Ng'anzo, U. Ryan, M. Olson, P. Cox, P. Monis, and R. Thompson.** 2004. Complete development of *Cryptosporidium parvum* in host cell-free culture. Int. J. Parasitol. **34:**769-777. doi: 10.1016/j.ijpara.2004.04.001.

29. **Hill, D. R., and T. E. Nash.** 2009. *Giardia lambliaIn* G. L. Mandell, J. E. Bennett, and R. Dolin (eds.), Mandell, Douglas and Bennett's Principles and Practices of infectious diseases, 7th ed., . Churchill livingstone, New York.

30. **Hur, S. C., T. Z. Brinckerhoff, C. M. Walthers, J. C. Dunn, and D. Di Carlo.** 2012. Label-free enrichment of adrenal cortical progenitor cells using inertial microfluidics. PloS One. **7:**e46550.

31. **Karanis, P., C. Kourenti, and H. Smith.** 2007. Waterborne transmission of protozoan parasites: A worldwide review of outbreaks and lessons learnt. Journal of Water and Health. **5:**1-38. doi: 10.2166/wh.2006.002.

32. **Keister, D.** 1983. Axenic culture of *Giardia lamblia* in TYI-S-33 medium supplemented with bile. Trans. R. Soc. Trop. Med. Hyg. **77:**487-488. doi: 10.1016/0035-9203(83)90120-7.

33. **Klotz, B., P. Manas, and B. M. Mackey.** 2010. The relationship between membrane damage, release of protein and loss of viability in *Escherichia coli* exposed to high hydrostatic pressure. Int. J. Food Microbiol. **137:**214-220. doi: 10.1016/j.ijfoodmicro.2009.11.020.

34. **Korich, D., J. Mead, M. Madore, N. Sinclair, and C. Sterling.** 1990. Effects of ozone, chlorine dioxide, chlorine, and monochloramine on *Cryptosporidium parvum* oocyst viability. Appl. Environ. Microbiol. **56:**1423-1428.

35. **Kotloff, K. L., J. P. Nataro, W. C. Blackwelder, D. Nasrin, T. H. Farag, S. Panchalingam, Y. Wu, S. O. Sow, D. Sur, R. F. Breiman, A. S. G. Faruque, A. K. M. Zaidi, D. Saha, P. L. Alonso, B. Tamboura, D. Sanogo, U. Onwuchekwa, B. Manna, T. Ramamurthy, S. Kanungo, J. B. Ochieng, R. Omore, J. O. Oundo, A. Hossain, S. K. Das, S.**

Ahmed, S. Qureshi, F. Quadri, R. A. Adegbola, M. Antonio, M. J. Hossain, A. Akinsola, I. Mandomando, T. Nhampossa, S. Acacio, K. Biswas, C. E. O'Reilly, E. D. Mintz, L. Y. Berkeley, K. Muhsen, H. Sommerfelt, R. M. Robins-Browne, and M. M. Levine. 2013. Burden and aetiology of diarrhoeal disease in infants and young children in developing countries (the Global Enteric Multicenter Study, GEMS): a prospective, case-control study. Lancet. **382:**209-222. doi: 10.1016/S0140-6736(13)60844-2.

36. **Lane, S., and D. Lloyd.** 2002. Current trends in research into the waterborne parasite *Giardia*. Crit. Rev. Microbiol. **28:**123-147.

37. **Le Goff, L., S. Khaldi, L. Favennec, F. Nauleau, P. Meneceur, J. Perot, J. -. Ballet, and G. Gargala.** 2010. Evaluation of water treatment plant UV reactor efficiency against *Cryptosporidium parvum* oocyst infectivity in immunocompetent suckling mice. J. Appl. Microbiol. **108:**1060-1065. doi: 10.1111/j.1365-2672.2009.04509.x.

38. **Leder, K., and P. F. Weller.** 2011. Epidemiology, clinical manifestations, and diagnosis of giardiasis. 2014**:** http://www.uptodate.com/contents/epidemiology-clinical-manifestations-and-diagnosis-of-giardiasis

39. **Lee, M. G., J. H. Shin, C. Y. Bae, S. Choi, and J. Park.** 2013. Label-free cancer cell separation from human whole blood using inertial microfluidics at low shear stress. Anal. Chem. **85:**6213-6218.

40. **Leitch, G. J., and Q. He.** 2012. Cryptosporidiosis-An overview. Journal of Biomedical Research. **25:**1-16.

41. **Liang, Z., and A. Keeley.** 2012. Comparison of propidium monoazide-quantitative PCR and reverse transcription quantitative PCR for viability detection of fresh *Cryptosporidium* oocysts following disinfection and after long-term storage in water samples. Water Res. **46:**5941-5953. doi: 10.1016/j.watres. 2012.08.014.

42. **Lim, E. J., T. J. Ober, J. F. Edd, G. H. McKinley, and M. Toner.** 2012. Visualization of microscale particle focusing in diluted and whole blood using particle trajectory analysis. Lab on a Chip. **12:**2199-2210. doi: 10.1039/c2lc21100a.

43. **Lindsay, D. S., B. L. Blagburn, and S. J. Upton.** 1999. Animal models of *Cryptosporidium* gastrointestinal infection, p. 851. *In* O. Zak and M. A. Sande (eds.), Handbook of Animal Models of Infection. Academic Press, San Diego, California.

44. **Lindsay, D. S., D. Holliman, G. J. Flick, D. G. Goodwin, S. M. Mitchell, and J. P. Dubey.** 2008. Effects of high pressure processing on *Toxoplasma gondii* oocysts on raspberries. J. Parasitol. **94:**757-758.

45. **Liu, L., H. L. Johnson, S. Cousens, J. Perin, S. Scott, J. E. Lawn, I. Rudan, H. Campbell, R. Cibulskis, M. Li, C. Mathers, R. E. Black, WHO, and UNICEF.** 2012. Global,

regional, and national causes of child mortality: an updated systematic analysis for 2010 with time trends since 2000. Lancet. **379:**2151-2161. doi: 10.1016/S0140-6736(12)60560-1.

46. **Majewska, A.** 1994. Successful experimental infections of a human volunteer and Mongolian gerbils with *Giardia* of animal origin. Trans. R. Soc. Trop. Med. Hyg. **88:**360-362. doi: 10.1016/0035-9203(94)90119-8.

47. **Matas, J., J. F. Morris, and É. Guazzelli.** 2004. Inertial migration of rigid spherical particles in Poiseuille flow. J. Fluid Mech. **515:**171-195.

48. **Mayrhofer, G., R. Andrews, P. Ey, M. Albert, T. Grimmond, and D. Merry.** 1992. The use of suckling mice to isolate and grow *Giardia* from mammalian fecal specimens for genetic-analysis. Parasitology. **105:**255-263.

49. **Mclaughlin, J.** 1993. The lift on a small sphere in wall-bounded linear shear flows. J. Fluid Mech. **246:**249-265. doi: 10.1017/S0022112093000114.

50. **Meyer, E.** 1970. Isolation and axenic cultivation of *Giardia* trophozoites from rabbit, chinchilla, and cat. Exp. Parasitol. **27:**179-&. doi: 10.1016/0014-4894(70)90023-8.

51. **Monteiro, L., D. Bonnemaison, A. Vekris, K. G. Petry, J. Bonnet, R. Vidal, J. Cabrita, and F. Megraud.** 1997. Complex polysaccharides as PCR inhibitors in feces: Helicobacter pylori model. J. Clin. Microbiol. **35:**995-998.

52. **Nam, S., and G. Lee.** 2010. A new duplex reverse transcription PCR for simultaneous detection of viable *Cryptosporidium parvum* oocysts and *Giardia duodenalis* cysts. Biomedical and Environmental Sciences. **23:**146-150.

53. **Oblath, E. A., W. H. Henley, J. P. Alarie, and J. M. Ramsey.** 2013. A microfluidic chip integrating DNA extraction and real-time PCR for the detection of bacteria in saliva. Lab on a Chip. **13:**1325-1332. doi: 10.1039/c3lc40961a.

54. **Olson, B. E., M. E. Olson, and P. M. Wallis.** 2002. *Giardia* The cosmopolitan parasite. CABI Publishing, New York, NY.

55. **Olson, M., J. Goh, M. Phillips, N. Guselle, and T. McAllister.** 1999. *Giardia* cyst and *Cryptosporidium* oocyst survival in water, soil, and cattle feces. J. Environ. Qual. **28:**1991-1996.

56. **Ozkumur, E., A. M. Shah, J. C. Ciciliano, B. L. Emmink, D. T. Miyamoto, E. Brachtel, M. Yu, P. I. Chen, B. Morgan, J. Trautwein, A. Kimura, S. Sengupta, S. L. Stott, N. M. Karabacak, T. A. Barber, J. R. Walsh, K. Smith, P. S. Spuhler, J. P. Sullivan, R. J. Lee, D. T. Ting, X. Luo, A. T. Shaw, A. Bardia, L. V. Sequist, D. N. Louis, S. Maheswaran, R. Kapur, D. A. Haber, and M. Toner.** 2013. Inertial focusing for tumor antigen-dependent and -independent sorting of rare circulating tumor cells. Sci. Transl. Med. **5:**179ra47. doi: 10.1126/scitranslmed.3005616; 10.1126/scitranslmed.3005616.

57. **Parichehreh, V., K. Medepallai, K. Babbarwal, and P. Sethu.** 2013. Microfluidic inertia enhanced phase partitioning for enriching nucleated cell populations in blood. Lab on a Chip. **13:**892-900.

58. **Petersen, R., and S. Lindquist.** 1989. Regulation of hsp70 synthesis by messenger-RNA degradation. Cell Regul. **1:**135-149.

59. **Rendtorff, R.** 1954. The experimental transmission of human intestinal protozoan parasites .2. *Giardia lamblia* cysts given in capsules. American Journal of Hygiene. **59:**209-220.

60. **Reynolds, O.** 1883. An experimental investigation of the circumstances which determine whether the motion of water shall be direct or sinuous, and the law of resistance in parallel channels. Proceedings of the Royal Society of London. 84.

61. **Ritossa, F.** 1996. Discovery of the heat shock response. Cell Stress Chaperones. **1:**97-98. doi: 10.1379/1466-1268(1996)001<0097:DOTHSR>2.3.CO;2.

62. **Robertson, L. J.** 2014. *Cryptosporidium* as a foodborne pathogen. Springer briefs in food, health and nutrition.

63. **Robertson, L., and B. Gjerde.** 2000. Isolation and enumeration of *Giardia* cysts, *Cryptosporidium* oocysts, and *Ascaris* eggs from fruits and vegetables. J. Food Prot. **63:**775-778.

64. **Robertson, L., and B. Gjerde.** 2001. Occurrence of parasites on fruits and vegetables in Norway. J. Food Prot. **64:**1793-1798.

65. **Robertson, L. J., and B. K. Gierde.** 2007. *Cryptosporidium* oocysts: challenging adversaries? Trends Parasitol. **23:**344-347. doi: 10.1016/j.pt.2007.06.002.

66. **Saffman, P.** 1965. Lift on a small sphere in a slow shear flow. J. Fluid Mech. **22:**385-&. doi: 10.1017/S0022112065000824.

67. **San Martin, M., G. Barbosa-Canovas, and B. Swanson.** 2002. Food processing by high hydrostatic pressure. Crit. Rev. Food Sci. Nutr. **42:**627-645.

68. **Santin, M., J. Trout, L. Xiao, L. Zhou, E. Greiner, and R. Fayer.** 2004. Prevalence and age-related variation of *Cryptosporidium* species and genotypes in dairy calves. Vet. Parasitol. **122:**103-117. doi: 10.1016/j.vetpar.2004.03.020.

69. **Scallan, E., R. M. Hoekstra, F. J. Angulo, R. V. Tauxe, M. Widdowson, S. L. Roy, J. L. Jones, and P. M. Griffin.** 2011. Foodborne illness acquired in the United States-Major Pathogens. Emerging Infectious Diseases. **17:**7-15. doi: 10.3201/eid1701.P11101.

70. **Schrader, C., A. Schielke, L. Ellerbroek, and R. Johne.** 2012. PCR inhibitors–Occurrence, properties and removal. J. Appl. Microbiol. **113:**1014-1026.

71. **Schupp, D., and S. Erlandsen.** 1987. Determination of *Giardia muris* cyst ciability by differential interference contrast, phase, or brightfield microscopy. J. Parasitol. **73:**723-729. doi: 10.2307/3282401.

72. **Segre, G., and A. Silberberg.** 1961. Radial particle displacements in Poiseuille flow of suspensions. Nature. **189:**209-&. doi: 10.1038/189209a0.

73. **Slifko, T., D. Freidman, J. Rose, and W. Jakubowski.** 1997. An *in vitro* method for detecting infectious *Cryptosporidium* oocysts with cell culture. Appl. Environ. Microbiol. **63:**3669-3675.

74. **Slifko, T., A. Coulliette, D. Huffman, and J. Rose.** 2000. Impact of purification procedures on the viability and infectivity of *Cryptosporidium parvum* oocysts. Water Science and Technology. **41:**23-29.

75. **Slifko, T., E. Raghubeer, and J. Rose.** 2000. Effect of high hydrostatic pressure on *Cryptosporidium parvum* infectivity. J. Food Prot. **63:**1262-1267.

76. **Smith, H. V., and R. A. B. Nichols.** 2010. *Cryptosporidium*: Detection in water and food. Exp. Parasitol. **124:**61-79. doi: 10.1016/j.exppara.2009.05.014.

77. **Smith, H., R. Nichols, and A. Grimason.** 2005. *Cryptiosporidium* excystation and invasion: getting to the guts of the matter. Trends Parasitol. **21:**133-142. doi: 10.1016/j.pt.2005.01.007.

78. **Tanaka, T., T. Ishikawa, K. Numayama-Tsuruta, Y. Imai, H. Ueno, N. Matsuki, and T. Yamaguchi.** 2012. Separation of cancer cells from a red blood cell suspension using inertial force. Lab on a Chip. **12:**4336-4343.

79. **Uga, S., J. Matsuo, E. Kono, K. Kimura, M. Inoue, S. Rai, and K. Ono.** 2000. Prevalence of *Cryptosporidium parvum* infection and pattern of oocyst shedding in calves in Japan. Vet. Parasitol. **94:**27-32. doi: 10.1016/S0304-4017(00)00338-1.

80. **Umemiya, R., M. Fukuda, K. Fujisaki, and T. Matsui.** 2005. Electron microscopic observation of the invasion process of *Cryptosporidium parvum* in severe combined immunodeficiency mice. J. Parasitol. **91:**1034-1039. doi: 10.1645/GE-508R.1.

81. **Upton, S., M. Tilley, M. Nesterenko, and D. Brillhart.** 1994. A simple and reliable method of producing *in vitro* infections of *Cryptosporidium parvum* (Apicomplexa). FEMS Microbiol. Lett. **118:**45-49. doi: 10.1016/0378-1097(94)90594-0.

82. **US Food and Drug Administration.** 2011. Kinetics of microbial inactivation for alternative food processing technologies -- High pressure processing. 2014:http://www.fda.gov/food/food scienceresearch/safepracticesforfoodprocesses/ucm101456.htm

83. **Vasseur, P., and R. Cox.** 1976. Lateral migration of a spherical-particle in 2-dimensional shear flows. J. Fluid Mech. **78:**385-413. doi: 10.1017/S0022112076002498.

84. **Vetterli.jm, A. Takeuchi, and P. Madden.** 1971. Ultrastructure of *Cryptosporidium wrairi* from Guinea Pig. J. Protozool. **18:**248-&. doi: 10.1111/j.1550-7408.1971.tb03316.x.

85. **Woodmansee, D.** 1987. Studies of *in vitro* excystation of *Cryptosporidium parvum* from calves. J. Protozool. **34:**398-402. doi: 10.1111/j.1550-7408.1987.tb03199.x.

86. **Wu, Z., B. Willing, J. Bjerketorp, J. K. Jansson, and K. Hjort.** 2009. Soft inertial microfluidics for high throughput separation of bacteria from human blood cells. Lab on a Chip. **9:**1193-1199.

87. **Yang, S.-Y., K.-Y. Lien, K.-J. Huang, H.-Y. Lei, and G.-B. Lee.** 2008. Micro flow cytometry utilizing a magnetic bead-based immunoassay for rapid virus detection. Biosensors and Bioelectronics. **24**: 855-862.

88. **Zhou, J., and I. Papautsky.** 2013. Fundamentals of inertial focusing in microchannels. Lab on a Chip. **13:**1121-1132.

CONTRIBUTIONS OF COLLABORATORS

All work pertaining to the design and fabrication of all versions of the microfluidic inertial separation chips, the design and set up of the pumping system, and development of the majority of the pumping protocols, was performed by our collaborators; Drs. Teodor Veres and Liviu Clime and the team at the Life Science Division of National Research Council Canada in Boucherville, Quebec.

APPENDIX I

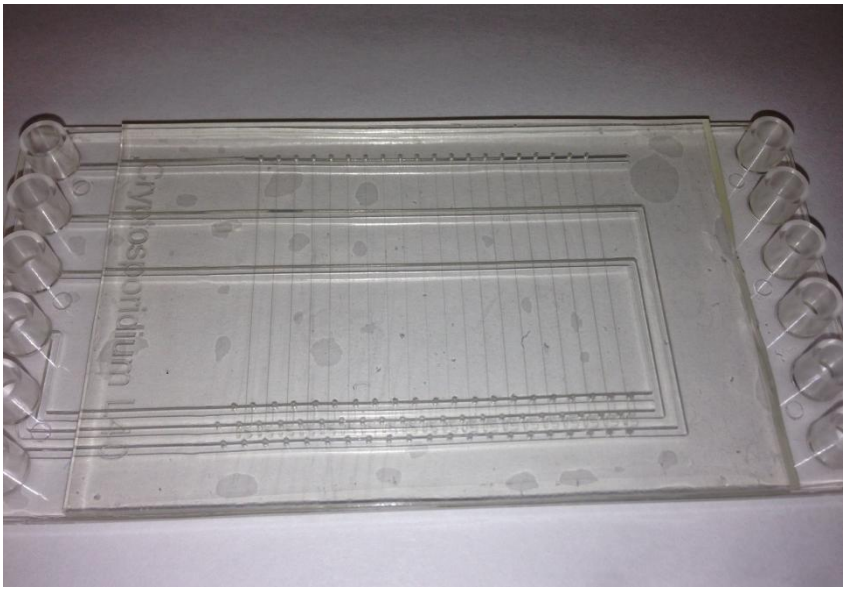

Third version of the *Cryptosporidium* microfluidic inertial separation chip containing 20 separation channels in parallel.